Utrecht University - KWR Water Research Institute

The impact of storage conditions and aquifer heterogeneity on Aquifer Storage Recharge (ASR) system's performance

José Luis Cifuentes Pérez
6569137

Utrecht University supervisor:

Alraune Zech

KWR supervisor:

Niels Hartog

MSc Earth Surface and Water
Department of Physical Geography
Faculty of Geosciences
Utrecht University

May 15, 2023

Abstract

Aquifer Storage and Recovery systems (ASR) are an alternative source of fresh water to the increasing demand for water. Its performance varies in terms of flow parameters, aquifer conditions and transport processes. An axisymmetric 50 m thick base model is defined to simulate ASR performance by using Modflow, MT3DMS and Seawat. The heterogeneous setting is defined as an alternation of high-K and low-K layers, where different hydraulic conductivities, contrast ratios and anisotropy factors are simulated for homogeneous and heterogeneous cases. Under the numerical approach the anisotropy factor in the homogeneous cases is the independent variable, while in the geological approach, the heterogeneous layers are the independent variable. The numerical approach makes different scenarios comparable and has a greater impact on the high-K layers' vertical conductivity K_V while the geological approach leads to realistic simulations and has a greater impact on the low-K layers' K_V. Higher values of K_V lead to a greater buoyancy effect and tilting of the fresh-naive water interface. Homogeneous cases have a better performance than heterogeneous cases, mainly during the first years of simulation. Peaks on RE after 4 or 6 years of simulation in heterogeneous cases can be explained by the transfer of fresh water to a high-K layer from an underneath low-K or high-K layer due to buoyancy. Homogeneous cases have a better performance than heterogeneous cases. RE is more impacted by K_V than horizontal hydraulic conductivity K_H, as it controls the amount of buoyancy. In heterogeneous cases, buoyancy in high-K layers is the main responsible for the reduction in RE compared to the homogeneous equivalent cases.

Keywords: ASR, heterogeneity, recovery efficiency, hydraulic conductivity, buoyancy.

A Julieta y Andrea

Contents

List of Figures

List of Tables

1 Introduction

Generalities

The increasing demand for drinking water and its reduced availability has made our society look for new ways to obtain and store freshwater. As society grows, more water is needed both for drinking water and industrial processes. In this context, the *water footprint*, which is an indicator of freshwater used to produce a product over its full supply chain [*Aldaya et al.*, 2012], has steadily increased over the last years. Population growth demands not just water itself, but also energy, which requires large amounts of water to be produced [*Spang et al.*, 2014]. Current and projected freshwater limitations would lead to a reduction of the irrigated areas, and later less food production, while just a few places would experience an increase of irrigation [*Elliott et al.*, 2014].

To face the challenge of increasing demand, several new techniques have been developed with the aim of increasing freshwater availability during the last decades. Among these techniques are seawater desalination [*Curto et al.*, 2021], fog collection [*Molina et al.*, 2008], rain water harvesting [*Campisano et al.*, 2017; *Pandey et al.*, 2021], coastal aquifer infiltration (COASTAR, *Essink et al.* [2018]) and Aquifer Storage Recovery (ASR) [*Brown et al.*, 2016; *Kaushal et al.*, 2020; *Li et al.*, 2021; *Lu et al.*, 2011; *Maliva et al.*, 2006; *Page et al.*, 2017; *Pavelic et al.*, 2006; *Ward et al.*, 2008; *Zuurbier et al.*, 2013, 2016].

Aquifer Storage and Recovery system

This project focuses on ASR systems, which are defined as *'the storage of water in a suitable aquifer through a well during times when water is available, and recovery of the water during times when it is needed'* [*Pyne*, 1995]. ASR can be used for seasonal storage, long-term storage or emergency storage. It is mainly applied when low hydraulic conductivity soils don't allow infiltration to the water table, when land availability is cost limited, or when surface recharge is not possible [*Pyne*, 1995]. The freshwater stored in ASR systems is often referred as *'freshwater bubble'* [*Maliva et al.*, 2005].

ASR is classified into two basic types: (i) physically bounded ASR, where water is stored in freshwater aquifers by increasing water pressure. The boundaries of the freshwater bubble in this type of system are equal to the aquifer boundaries ; and (ii) chemically bounded ASR. In the latter, the freshwater is injected into an aquifer of poor-quality water by displacing it. The boundary of the freshwater bubble is the fresh-saltwater interface. Injected water in ASR systems enters preferentially in high hydraulic conductivity layers (high-K layers), while low hydraulic conductivity layers (low-K) remain hosting native water. In the same way, during the pumping phase, high-K layers contribute with a higher volume of water than the low-K layers for the whole system. The recovery targets on the minimal mixing with native formation waters [*Maliva et al.*, 2005].

A cycle is the period of time between two injection phases, which usually is 1 year. Each cycle is divided into *injection phase*, *storage phase*, *recovery phase* and *inactive phase*. They can be described as follows: (i) During the *injection phase* freshwater is injected typically over 91 days. It is based on the assumption of a water surplus during that period. (ii) During the *storage phase* freshwater is stored in the aquifer over 91 days. (iii) During the *recovery phase* freshwater is pumped out over 91 days or until the *cutoff* is reached. The cutoff concentration is a quality criterion of salt content in water based on the assumption of a certain quality of water is needed. In this project, this limit is set equal to the chloride concentration in Dutch drinking water, 0.5 *g/l*. (iv) During the *inactive phase* the remaining freshwater stays in the aquifer.

The performance of the ASR system is determined by the *recovery efficiency* (RE), defined as *'the percentage of the water volume stored that is subsequently recovered while meeting a target water quality criterion in the recovered water'* [*Pyne*, 1995]. It can be expressed by the following relationship [*Ward et al.*, 2007]:

$$RE = \frac{V_{out}}{V_{in}} \tag{1}$$

where V_{in} is the injected volume of freshwater and V_{out} is the recovered volume of water.

In the presence of significant water density differences, e.g. between injected freshwater and native saltwater, injected water flows upward due to buoyancy [*Maliva et al.*, 2005; *Li et al.*, 2021]. This results in a tilting of the fresh-saline water interface, increasing salinity at the bottom and decreasing salinity at the top. Longitudinal dispersion contributes to the mixing of fresh and saline water, creating a brackish mixing zone. Both processes, interface tilting and dispersion in the mixing zone, become more significant in high-K layers [*Li et al.*, 2021].

Another way to describe the ASR systems is by the mixing fraction (M_f). *Zuurbier et al.* [2013] defines it as *the proportion of injected water in the recovered water as a function of time during recovery*, expressed as:

$$M_f = \frac{S_{native} - S_{recovered}}{S_{native} - S_{injected}} \tag{2}$$

where S_{native} is the salt concentration of the native groundwater, $S_{recovered}$ is the salt concentration of the recovered water, $S_{injected}$ is the salt concentration of the injected water. Thus, M_f has a value of 1 at the beginning of the injection phase, but it decreases during the recovery phase.

Modelling the spread of the *freshwater bubble* in real aquifers is more complex due to the inherent aquifers heterogeneity. The heterogeneity is understood as the arrangement of layers with different hydraulic conductivities in an aquifer, represented in this project by the alternation of high-K and low-K layers in the aquifer profile. Interfingering among freshwater in high-K layers and brine in low-K layers is often present, developing an interface area. During the injection phase, the size of the interface area will be proportional to the hydraulic conductivity contrast between the two layers [*Maliva et al.*, 2005]. The same authors found that RE is reduced as the degree of heterogeneity in the aquifer increases. In addition, dispersion increases with velocity [*Barker*, 2007], so the performance of ASR systems is affected by diffusion/dispersion, both in the lateral interface (mixing zone) and in the vertical interface due to layer heterogeneity.

Despite advection being the main process in the ASR systems, changes in ASR performance induced by the heterogeneity still need to be assessed. In fact, as heterogeneity leads to an increment in the interface area, it leaves more room for diffusion to take place.

RE depends on the volume of recoverable water meeting the cutoff, so its value depends on the amount of mixing of freshwater and native water and on the aquifer's physical parameters. Given the importance that heterogeneity in the hydraulic conductivity field has on RE, it is important to know which level of accuracy and resolution of available information is required in layer's characterisation. *Li et al.* [2021] showed that assuming a homogeneous setting can result in an overestimation of RE. *Li et al.* [2022] has shown that heterogeneous settings have a worse RE performance than the homogeneous equivalent. Nevertheless, this gap is reduced over the iterated cycles.

Filling this gap of knowledge is important because real-world scenarios are not homogeneous, but aquifers are heterogeneous. Approaching the ASR system as a heterogeneous system can help to understand its behaviour by: (i) understanding which processes take place during the different phases and to what extent they take place, (ii) developing more realistic and precise scenarios, avoiding over and underestimations of RE.

Objectives and Research Questions

I will address the question of *What degree of characterisation is required to obtain a realistic RE in a heterogeneous layered system* by creating deterministic layered scenarios. To that end, I will use numerical modelling to analyse ASR systems and their performances (REs) under different hydrogeological conditions and under various levels of characterisation resolution.

The main objective is to determine the minimum characterisation resolution required to be incorporated in numerical models to obtain a realistic RE estimation in heterogeneous aquifer systems for different ASR system conditions. Specific objectives are:

1. Supply the construction of computationally efficient and realistic numerical models for the prediction of ASR performance based on recovery efficiency and optimized model design.
2. Establish guidelines to develop efficient aquifer characterization and implementation in numerical models.

Research questions are:

1. What level of detail in spatial heterogeneity in the form of layering is required to be incorporated in numerical models for different ASR storage conditions?
2. How do the levels of spatial heterogeneity vary for different hydrogeological conditions such as horizontal and vertical hydraulic conductivity, dispersivity, and diffusion coefficients?
3. How does the recovery efficiency depend on different operation and aquifer conditions such as storage volume, aquifer thickness, and native salinity?

2 Theoretical framework

Freshwater injected into the aquifer spreads differently depending on hydrogeological layer properties. The involved subsurface flow and transport processes are described in the following.

2.1 Flow, parameters and aquifer conditions

2.1.1 Darcy's law and hydraulic conductivity

Flow
The flow is the movement of water through a porous media. Its average linear velocity (v_x, also known as effective velocity) is the *rate at which the flux water across the unit cross-sectional area of pore space occurs* and can be expressed as follows:

$$v_x = \frac{K_x}{n_e}\frac{dh}{dx} \tag{3}$$

were v_x is the average linear velocity in the x direction $[L/T]$, K_x is the hydraulic conductivity in the x direction $[L/T]$, n_e is the effective porosity $[-]$ (the porosity through which flow can occur), and $\frac{dh}{dx}$ is the hydraulic gradient $[L/L]$ [*Fetter et al.*, 2018].

Darcy's law
The flow of water through porous media is described by Darcy's law:

$$Q = -K\frac{dh}{dx}A \tag{4}$$

were Q is the discharge flow rate $[L^3/T]$, K is the hydraulic conductivity $[L/T]$, dh/dx is the hydraulic gradient $[-]$, and A is the cross-sectional area of the medium $[L^2]$. The negative sign is required as the hydraulic head decreases in the direction of the flow [*Fitts*, 2002]. The hydraulic head is the potential energy of the water in the aquifer due to the elevation and pressure.

Hydraulic conductivity
The hydraulic conductivity (K) is the property of the medium which indicates how easily the water can be transferred through it [*Fitts*, 2002]. A high K material allows the passing of a larger amount of water through it than a low K material. The hydraulic conductivity has a wide range of values of about 14 orders of magnitude in geological materials, from shale to gravel (Figure 2.1). The *horizontal hydraulic conductivity* K_H is the ability of the porous media to transfer water horizontally, while the *vertical hydraulic conductivity* K_V is the ability of the porous media to transfer water vertically.

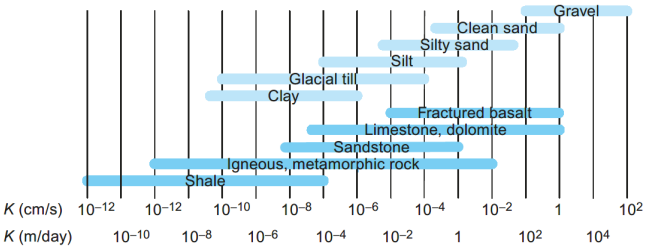

Figure 2.1: Range of values of hydraulic conductivity. Taken from *Fitts* [2002]

.

Anisotropy
A material is *isotropic* when K is equal in all spatial directions, i.e. $K_H = K_V$. A material is *anisotropic* when K varies in different directions, i.e. $K_H \neq K_V$ [*Fitts*, 2002]. The anisotropy is defined as the ratio between horizontal and vertical hydraulic conductivity [*Beernink et al.*, 2022]:

$$f_{ani} = \frac{K_H}{K_V} \tag{5}$$

were f_{ani} is the anisotropy factor, K_H is the horizontal hydraulic conductivity, and K_V is the vertical hydraulic conductivity. Usually, K_H is bigger than K_V due to burial and processes such as compaction and deposition, so the value of f_{ani} is greater than 1. This value goes from 2 to 3 in sand grains under typical package pressure and grain shape and up to 10 to 100 on the core scale to aquifer scale. The anisotropy is dependent on the scale of the measurement and increases with increasing scale [*Beernink et al.*, 2022].

Average hydraulic conductivity

In aquifers composed of multiple layers with different K values, but uniform per layer, the overall hydraulic conductivity is gained by different averaging strategies. The horizontal average horizontal hydraulic conductivity K_{H-av} of the sequence is represented by the arithmetic mean (Equation 6), while the vertical average hydraulic conductivity K_{V-av} is represented by the harmonic mean (Equation 7):

$$K_{H-av} = \frac{\sum_i K_{H-i}}{H_{tot}} \tag{6}$$

$$K_{V-av} = \frac{H_{tot}}{\sum_i \frac{H_i}{K_{V-i}}} \tag{7}$$

where K_{H-av} and K_{V-av} are the horizontal and vertical average hydraulic conductivity, respectively; K_{H-i} and K_{V-i} are the horizontal and vertical hydraulic conductivity of each layer i, respectively; and H_i is the thickness of layer i; and $H_{tot} = \sum_i H_i$ is the aquifer thickness [*Beernink et al.*, 2022].

Heterogeneity

A material is *heterogeneous* when K varies spatially [*Fitts*, 2002]. A schematic visualization of both concepts, anisotropy and heterogeneity is shown in Figure 2.2.

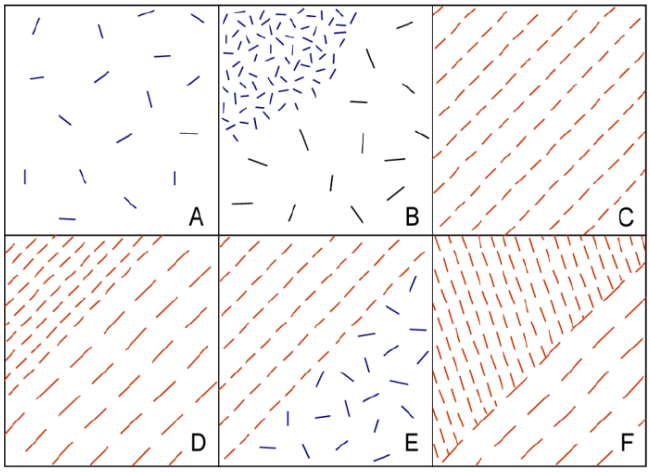

Figure 2.2: Schematic representation of anisotropy and heterogeneity in rock fabric. A) homogeneous and isotropic; B) Overall heterogeneous and isotropic, with two different homogeneous and isotropic areas; C) homogeneous and anisotropic; D) overall heterogeneous and anisotropic, with two different areas that are each homogeneous and anisotropic; E) overall heterogeneous, with one area that is homogeneous and isotropic, and one area that is homogeneous and anisotropic; F) overall heterogeneous and anisotropic. Taken from *Kresic* [2022].

Contrast ratio

In this project, the heterogeneous profiles are constructed as a binary model. It means that high-K layers and low-K layers are alternated over the profile. The ratio of contrast between the high-K and low-K layers is described by:

$$CR = \frac{K_{H-high}}{K_{H-low}} \tag{8}$$

were CR is the contrast ratio, K_{H-high} is the horizontal hydraulic conductivity of the high-K layers, and K_{H-low} is the hydraulic conductivity of the low-K layers. The lowest value of CR is 1, which occurs when high-K and low-K layers are identical (equivalent to the homogeneous setting).

Transmissivity
Transmissivity T $[L^2/T]$ is the measure of how easily a layer transmits water [*Fitts*, 2002]. It is described by:

$$T_i = K_i H_i \tag{9}$$

were K_i is the hydraulic conductivity of layer i, and h_i is the thickness of layer i. An aquifer has a high transmissivity when it has a high hydraulic conductivity and/or a large thickness [*Kresic*, 2022]. When a profile is composed of different layers, with different hydraulic conductivities K_i and thicknesses H_i, the overall transmissivity T is expressed as the sum of every layer transmissivity [*Fitts*, 2002]:

$$T = \sum_i T_i \tag{10}$$

2.1.2 Density and buoyancy

Density
The mass density of freshwater $\rho_{fw}[M/L^3]$ varies in a narrow range, between 0.998 to 1.000 $[g/cm^3]$ at temperatures between 0°C to 20°C under atmospheric pressure. The weight density equals the water mass density times the gravitational acceleration $g[L/T^2]$. It slightly varies with temperature, pressure, and chemical composition. The higher the temperature is, the less dense the fluid is, as the molecules move at major velocity overcoming molecular attraction forces [*Fitts*, 2002]. The linear relationship between chloride concentration and density is given by the expression:

$$\rho_{Cl} = \rho_f + 1.340 \cdot C_{amb} \tag{11}$$

were ρ_{Cl} is the saltwater density, ρ_f is the freshwater density and C_{amb} is the salinity of the water in the aquifer (Figure 2.3, *Zuurbier et al.* [2013]). In this project, the water salinity is represented by the chloride concentration.

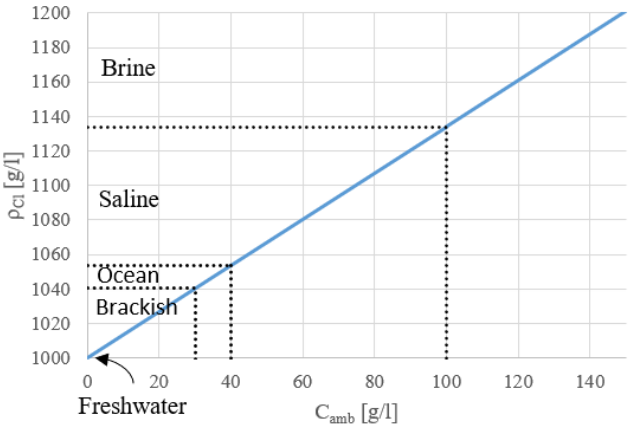

Figure 2.3: Linear relationship between chloride concentration and water density [*Zuurbier et al.*, 2013] and typical values of salinity of various water taken from *Fitts* [2002].

Density-effect
During the injection of less dense freshwater into an aquifer filled with denser native water, a vertical interface develops. This interface will tilt due to the interface instability driven by density differences (Figure 2.4). As a result, the initial cylindric freshwater bubble turns into a conical shape, wider at the top and narrow at the base and the RE is reduced [*Ward et al.*, 2007].

Nevertheless, other authors relate the interface tilting not just to density difference, but also to permeability (Merritt [1986], Missimer et al. [2002] and Yobbi [1996], in *Ward et al.* [2007]). Not recovered freshwater during the recovery phase depends on the mixing zone and the interface tilt. Free convection is driven by density gradient, while forced convection is caused by hydraulic gradient [*Ward et al.*, 2007].

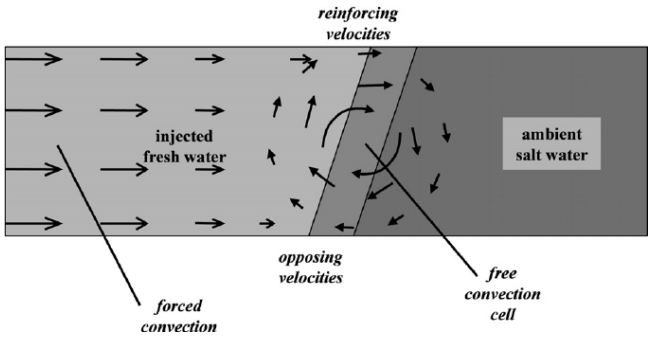

Figure 2.4: Schematic of free convection and forced convection. Taken from *Ward et al.* [2007].

2.2 Transport processes

2.2.1 Advection

Advection is the process that takes place when dissolved particles are carried along with the flowing groundwater. The amount of transported solute is a function of its concentration and the quantity of the groundwater flowing [*Fetter et al.*, 2018].

Pure advective transport leads to a sharp concentration front in the flow direction. In layered material, the travel distance in a given time span is greater in layers with higher hydraulic conductivity K, leading to a front spreading at different rates in each layer [*Fetter et al.*, 2018].

The mass flux of a solute due to advection can be expressed by:

$$F_{adv-x} = q_x C \tag{12}$$

were F_{adv-x} is the advective flux of solute mass in the x direction, q_x is the specific discharge in the x direction, and C is the solute concentration ($\frac{mass}{volume}$) [*Fitts*, 2002]

2.2.2 Diffusion

Diffusion is the process of *mixing that occurs due to the random motion of molecules in a fluid* [*Fitts*, 2002]. Diffusion moves solute mass from high-concentration areas to lower-concentration areas. This movement is independent of advection and is conceptually analogue to heat diffusion. The diffusive flux $F_{\text{diff-x}}$ is governed by Fick's law:

$$F_{\text{diff-x}} = -n_e \frac{D_{\text{mol}}}{\tau} \frac{dC(x)}{dx} \tag{13}$$

were n_e is the effective porosity of the medium, τ is the tortuosity, D_{mol} is the molecular diffusion coefficient, and $\frac{dC(x)}{dx}$ is the gradient of concentration.

Water in porous media occupies only a fraction of the whole space, leading to a slower molecular diffusion than in sole water. Tortuosity τ is a measurement of how tortuous the typical flow path is through the medium [*Fitts*, 2002]. It varies with the direction as the fabric of the porous medium varies with direction. It is expressed as [*Fitts*, 2002]:

$$\tau = \frac{L_e}{L} \tag{14}$$

were L_e is the actual (tortuous) travel length of the particle between two points, and L is the length of the shorter connection between the two points (straight line). As $L_e > L$, tortuosity is always greater than 1.

The molecular diffusion coefficient D_{mol} $[L^2/T]$ is a scalar property and depends on temperature and fluid properties, such as salinity. Particles move faster at higher temperatures, leading to a large D_{mol}. Similarly, smaller particles move faster. Conversely, the higher the viscosity the lower D_{mol}.

2.2.3 Dispersion

Dispersion is the spreading of solutes in porous media due to velocity fluctuations caused by the porous medium structure. It is based on three principles: fluids move faster at the centre of the pore than along the edges;

some particle paths are longer than others in the porous media to travel the same distance; particles can move faster through bigger pores than through small ones [*Fetter et al.*, 2018].

The effects of mechanical dispersion plus molecular diffusion are lumped together in hydrodynamic dispersion, governed by:

$$F_{mx} = -nD_{mx}\frac{dC}{dx} \tag{15}$$

were n is porosity, C is concentration, and D_{mx} is the hydrodynamic dispersion coefficient in the x direction consisting of mechanical dispersion and molecular diffusion:

$$D_{mx} = \alpha_l|\overline{v}|+\tau D_{mol} \tag{16}$$

were α_l is the longitudinal dispersivity, $|\overline{v}|$ is the magnitude of the average linear velocity of flow, τ is the tortuosity in the x direction, and D_{mol} is the molecular diffusion coefficient. In all but the lowest K materials like clays, mechanical dispersion causes more mixing than molecular diffusion, so the diffusive term is typically neglected.

2.2.4 Advection Dispersion Equation

The conservative transport of solutes is described by the advection-dispersion-equation (ADE) which combines the processes of advection and hydrodynamics:

$$\frac{dC}{dt} + v \cdot \nabla C - \nabla \cdot (D_m \nabla C) = r_{sink/source} \tag{17}$$

where $\frac{dC}{dt}$ is the change of concentration over time, v is the groundwater velocity (Darcy's velocity), C is the concentration, ∇ is the gradient operator, D_m is the dispersion and $r_{sink/source}$ describes a sink or source of concentration.

3 Model

The research questions are addressed through numerical groundwater flow and transport simulations with Modflow [*Harbaugh*, 2005], MT3DMS [*Bedekar et al.*, 2016], and Seawat [*Guo and Langevin*, 2002] packages in the Python environment flopy [*Bakker et al.*, 2016] to solve equations (3), (4), (12), (13), (15) and (17). I used an axisymmetric model created by *Beernink* [2019] to analyse Aquifer Thermal Energy Storage (ATES) systems. Based on the premise that thermal and mass transfer processes are similar, *Lentz* [2023] modified the model to investigate the influence of buffer value in ASR systems, for homogeneous aquifers. A deterministic approach of heterogeneity was included to the model, where the aquifer is subdivided into 3, 6, 9, 10 or 20 layers with different hydraulic conductivities.

The homogeneous settings are defined by a single layer with a given horizontal and vertical hydraulic conductivity. Heterogeneous settings are defined by the alternation of several layers with different horizontal and vertical hydraulic conductivity. The total thickness of the layers in the heterogeneous setting is 50 m, equal to the single layer of the homogeneous case.

3.1 Numerical model setup

3.1.1 Axisymmetric model

An axisymmetric model is an alternative to a full 3D model to calculate flow and transport in a well setting causing radial symmetric pattern. It is about 1000 times faster than its equivalent 3D model due to the reduction of the governing equations to two dimension [*Langevin*, 2008]. The regional hydraulic gradient is discarded in this model, so the recovered or injected water moves radially under homogeneous conditions.

The finite-difference grid of the axially symmetric model is determined by the horizontal cell width $y-$axis, which increases away from the well; the cell thickness $z-$axis, which is positive in the upward direction (Figure 3.1a). The model assumes a confined aquifer. Transmissivity T of all layer is the product of the hydraulic conductivity (K) and its thickness (dz).

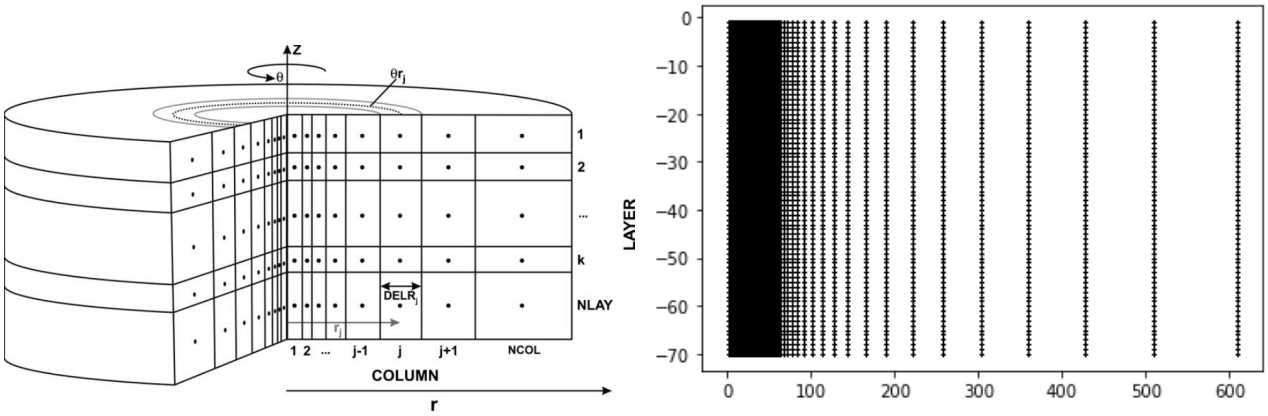

Figure 3.1: (a) Schematic of an axially symmetric profile model. j and k indices are columns and rows, respectively. Taken from *Langevin* [2008]. (b) Project grid profile.

3.1.2 Spatial and temporal settings

The axial symmetric grid is defined with the injection-recovery well at the left, so the injected freshwater spreads to the right-hand side (Figure 3.1b). The cell size in the horizontal plane increases from 0.5 m at the well for the first 100 cells, up to 100 m at the boundary at 610 m. The vertical grid size is 1 m but a few simulations were carried out with a vertical grid size of 0.5 m.

The *coupled simulation* is the base of the temporal setting, where the time period is 1 d, the number of Modflow stress periods is one and the number of Modflow time steps per stress period is one. Cycles are composed of 365 coupled simulations run for one and ten years (cycles).

A stopping criterion (cutoff) is checked after every coupled simulation to evaluate during the recovery phase whether to continue or stop the extraction. The model starts in winter (to set surface temperature) but it does not impact results. The simulations were run under steady-state conditions. The recovery efficiency has discrete

increments of 1.1% equivalent to one day of extraction after 91 days of injection. We will refer to this as the *time resolution*.

The salinity of the hosting aquifer remains constant and does not change over the simulation. The groundwater flow velocity in all directions is neglected (set to 0 m/d). Water density is considered variable for the simulations with buoyancy but constant otherwise. Temperature is constant in the whole model domain. Simulations were set in a confined aquifer.

3.2 Base simulation

The input parameters of the model can be classified into aquifer properties, water properties and ASR properties (Table 3.1). The aquifer is confined by an aquitard layer both at the top and bottom of the model. The aquitards have a very low horizontal hydraulic conductivity $K_h = 0.05\ m/d$ and a thickness of 10 m. The aquifer has a total thickness of 50 m for the homogeneous case. It is divided into 10 layers of 5 m each for the heterogeneous cases (Figure 3.2). For the heterogeneous cases, a binary setting is defined, where high and low hydraulic conductivity layers (high-K and low-K, respectively) are systematically alternated. They are represented by the contrast ratio CR. Every heterogeneous setting has a respective homogeneous equivalent case. The conductivities of the homogeneous case are defined by the horizontal and vertical average hydraulic conductivity, as in Equations (6) and (7), respectively.

Table 3.1: Aquifer, water and ASR parameters in numerical simulations

Aquifer				**Water**		**ASR**	
Property	**Value**	**Property**	**Value**	**Property**	**Value**	**Property**	**Value**
Layers	10	Dispersivity	0.1 m	Native water salinity	5 g/l	Injected water volume	50000 m^3
$K_{H-average}$	5 m/d	α_v/ α_l	0.001 m	Temperature	10 ° C	Injection flow	549 m^3/d
Contrast ratio	5	Molecular diffusion coefficient	10^{-9} m^2/s	Water density	1000 g/l	Cutoff	0.15 g/l
Anisotropy	5	Specific storage	6 10^{-4} m^{-1}			Injected water salinity	0 g/l
Thickness	50 m	Effective porosity	0.3				

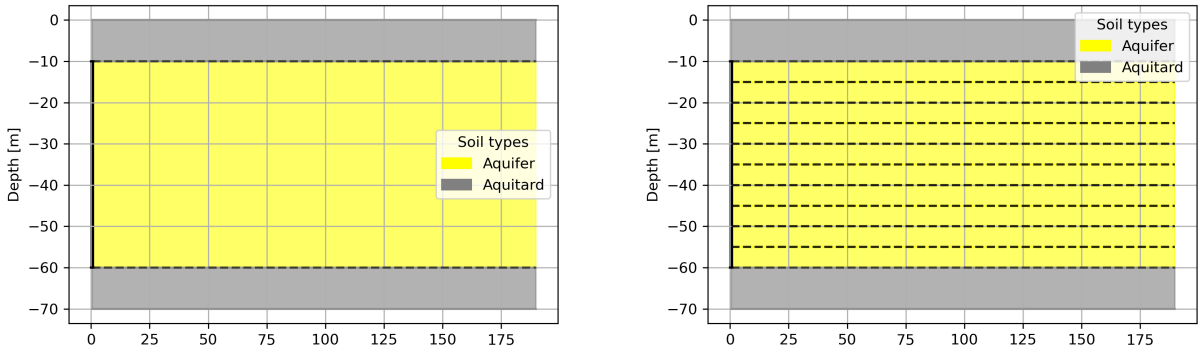

Figure 3.2: Profiles for the base simulations: (a) homogeneous case, 50 m thick layer; (b) heterogeneous 10 layers case, 5 m thick each and 50 m thick in total. The pumping well is located at the left-hand side of the profiles.

3.3 Approaches for vertical conductivity and anisotropy

Homogeneous and heterogeneous cases were set to be equivalent in order to make them comparable. This equivalence was built up by controlling the horizontal and vertical hydraulic conductivity under different scenarios, both for homogeneous equivalent and heterogeneous cases.

Homogeneous equivalent hydraulic conductivities are the average heterogeneous hydraulic conductivities, based on equations (6) and (7), respectively (Table 3.2). In heterogeneous cases, the average horizontal hydraulic conductivity is defined as an independent variable. The layers' horizontal hydraulic conductivity is defined as a dependent variable in terms of the average horizontal hydraulic conductivity and the contrast ratio. Therefore, the vertical hydraulic conductivities K_V and anisotropy factor adopt different values in order to fit with the desired K_H and contrast ratio simulated. After defining the horizontal hydraulic conductivity for homogeneous and heterogeneous cases, two ways to determine anisotropy and vertical hydraulic conductivity are proposed: the numerical and the geological approach.

Table 3.2: Hydraulic conductivities K and anisotropy factor f_{ani} for the numerical and geological approaches in binary simulations. Geological approach is divided into $f_{ani} = 2$ and $f_{ani} = 5$. Parameters are included as independent (green) and as dependent (yellow). Abbreviations: contrast ratio CR, horizontal hydraulic conductivity K_H, vertical hydraulic conductivity K_V. Horizontal average hydraulic conductivity is obtained by Equation (6) and the vertical average hydraulic conductivity by Equation (7).

	Numerical approach				**Geological approach**							
					$f_{ani} = 5$				$f_{ani} = 2$			
CR		K_H [m/d]	K_V [m/d]	f_{ani}		K_H [m/d]	K_V [m/d]	f_{ani}		K_H [m/d]	K_V [m/d]	f_{ani}
10	**High-K layer**	9.09	5.50	1.65	**High-K layer**	9.09	1.82	5.00	**High-K layer**	9.09	4.55	2.00
	Low-K layer	0.91	0.55		**Low-K layer**	0.91	0.18		**Low-K layer**	0.91	0.45	
	K average	5.00	1.00	5.00	**K average**	5.00	0.33	15.13	**K average**	5.00	0.83	6.05
100	**High-K layer**	9.90	50.50	0.20	**High-K layer**	9.90	1.98	5.00	**High-K layer**	9.90	4.95	2.00
	Low-K layer	0.10	0.51		**Low-K layer**	0.10	0.02		**Low-K layer**	0.10	0.05	
	K average	5.00	1.00	5.00	**K average**	5.00	0.04	127.51	**K average**	5.00	0.10	51.01

3.3.1 Numerical approach

In the numerical approach, the homogeneous f_{ani} is the independent variable while the heterogeneous layers' f_{ani} is the dependent variable. The heterogeneous layers' vertical conductivity are normalized to obtain an average vertical conductivity identical to the homogeneous vertical conductivity. As a consequence, the degree of change in the anisotropy of the heterogeneous layers is controlled by the contrast ratio CR, where the higher the CR is, the smaller the layers' f_{ani} become. Scenarios with the same heterogeneous average conductivity but different CR lead to the same homogeneous equivalent scenario. Thus, simulations with different CR can be comparable. Nevertheless, this can lead to unrealistic scenarios where K_H is smaller than K_V (f_{ani} smaller than 1).

3.3.2 Geological approach

In the geological approach, the heterogeneous layers' f_{ani} are the independent variables while the homogeneous f_{ani} are the dependent variables. The heterogeneous layers' vertical conductivity K_V are obtained from the normalized layers' horizontal conductivity K_H by using a constant anisotropy factor f_{ani}. The average vertical conductivity and homogeneous vertical conductivity are variable. The higher the CR, the smaller is homogeneous f_{ani}. This approach is more realistic as the anisotropy values in the heterogeneous layers remain realistic. The layers' f_{ani} were simulated for values of two and five. Scenarios with different CR lead to different average vertical conductivities making them less comparable.

3.4 Scenarios

A scenario corresponds to a simulation where at least one parameter is set differently than for the base simulation (Table 3.1). The variable parameters are: number of layers, average horizontal hydraulic conductivity K_{H-av}, contrast ratio CR, anisotropy factor f_{ani}, native water salinity C_{native}, injected water volume V and cutoff. The variable properties are applied to the heterogeneous and the homogeneous equivalent cases, resulting in (at

least) two scenario cases. All these scenarios are simulated with buoyancy and some scenarios without buoyancy to test its effect. The salinity of the native water in the aquifer C_{native} is variable for different scenarios, with a range from 2 to 50 $[g/l = kg/m^3]$.

Most of the heterogeneous settings were simulated for 10 layers, but some for 20, 9, 6 and 3 layers. For the 20 layer setting, the aquifer was divided into alternating layers of 3 m and 2 m thicknesses to complete the overall 50 m aquifer. In addition, the aquifer was divided into 3 layers, then subdivided into 6 layers and later subdivided again into 9 layers. Nevertheless, the thickness of that layer setting was completely arbitrary to keep a total thickness of 50 m aquifer. Simulated scenarios were classified by the type of approach and later by the changing parameters (Table 3.3).

Table 3.3: Simulated scenarios and parameters under the numerical and geological approaches. Abbreviations: average horizontal hydraulic conductivity K_{H-av}, contrast ratio CR, native water salinity C and anisotropy factor f_{ani}.

Numerical approach				**Geological approach**			
Scenario	K_{H-av}	CR	C	Scenario	CR	f_{ani}	Case
A1	5	10	5	B1	10	5	Homo
A2	5	10	10	B2	10	5	Hete
A3	10	10	10	B3	100	5	Homo
A4	10	10	5	B4	100	5	Hete
A5	5	100	5	B5	1	5	Homo
A6	10	100	5	B6	1	2	Hete
A7	5	100	10	B7	10	2	Hete
A8	10	100	10	B8	100	2	Hete
A9	5	1	5	B9	10	2	Homo
				B10	100	2	Homo
				B11	1	2	Homo
				B12	50	2	Homo
				B13	50	2	Hete

3.4.1 Fresh water bubble in a binary setting layer over 1-year simulation

One-year simulations were run to observe the behaviour of the freshwater bubble during the four phases of one cycle. The simulation is for 10 layers model and includes a buoyancy and a no buoyancy case. Simulations were carried out under the numerical approach.

3.4.2 Binary heterogeneous setting over 10 cycles for 10 layers: salinity and hydraulic conductivity variable

The model was run under aquifer salinities of 5 and 10 $[g/l]$ and hydraulic conductivities of 5 and 10 $[m/d]$ for a 10-layers setting. Furthermore, a scenario with no buoyancy was modelled for each case. All the parameters set for this scenario are summarized in Table 3.3. Simulations were carried out under the numerical approach.

3.4.3 Variable layers and variable parameters: salinity, injected volume cutoff and hydraulic conductivity

One-year simulations were carried for 3, 6 and 9 layers (Figures 3.3c, d, and e). The definition of layering was based on the subdivision of the aquifer into 3 layers and the subsequent subdivision into 6 and 9 layers. Nevertheless, this method is arbitrary. A reference scenario of native water salinity of 2 g/l, injected volume of 50,000 m^3 and a cutoff concentration of 0.15 g/l was set to compare against variable parameters to explore their influence on RE. Different values of native water salinity, injected volume and cutoff concentration were simulated. Simulations were carried out under the numerical approach.

3.4.4 Different hydraulic conductivity approaches: average constant or layer constant

Numerical and geological approaches are compared for the contrast ratios of 10 and 100. The horizontal hydraulic conductivity is 5 m/s and the native water salinity is 5 g/l. Nevertheless, homogeneous and heterogeneous cases

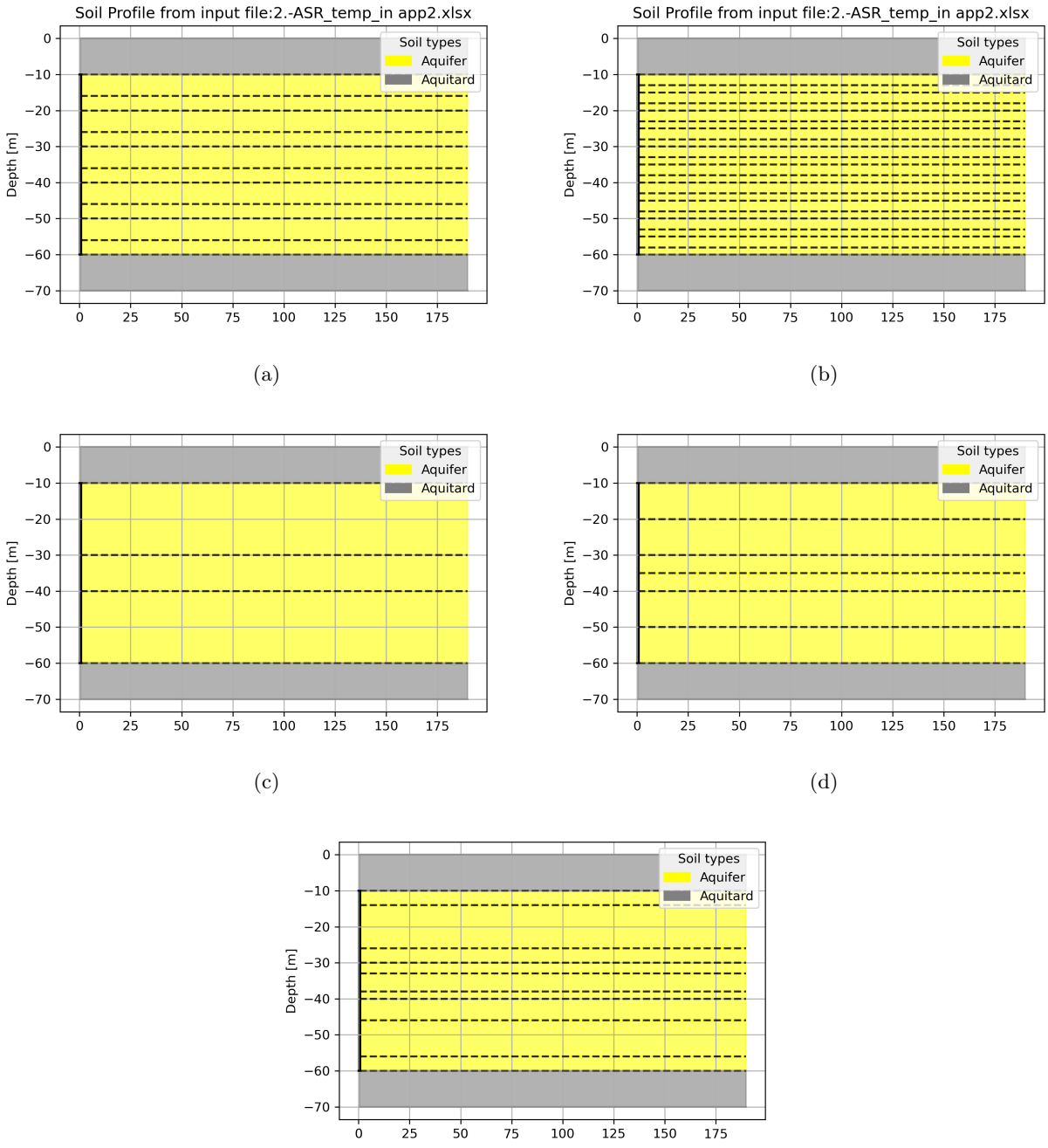

Figure 3.3: Profiles for different not the base cases simulated scenarios: (a) heterogeneous 10 layers alternating 6 m and 4 m thickness layers; (b) heterogeneous 20 layers alternation of 3 m and 2 m thickness layers; (c) 3 layers profile; (d) 6 layers profile; and (e) 9 layers profile. Arranges (a) and (b) are used in section 3.5 and 4.2.3. Arranges (c), (d) and (e) are used in section 4.1.3.

are not 100 % comparable, as always some differences are present (section 3.3). Simulations were carried out with buoyancy and without buoyancy. All the parameters set for this scenario are summarized in Table 3.3.

3.4.5 Anisotropy factor: 2 vs 5

The anisotropy factor in non-consolidated sand is about 2-3, while in core scales can be increased to 10-100 [*Beernink et al.*, 2022]. The anisotropy factor f_{ani} of 5 and 2 are compared under the geological approach. It is comparing homogeneous and heterogeneous cases and the respective no buoyancy cases. All the parameters set for this scenario are summarized in Table 3.3.

3.4.6 Contact area

Simulations with 20 layers were carried out to explore further performances in RE with alternating thicknesses of 3 $[m]$ and 2 $[m]$ (Figure 3.3b). An alternation of 6 $[m]$ and 4 $[m]$ thicknesses was simulated for the 10 layers simulation (Figure 3.3a). The homogeneous case is equivalent to the 10 and 20 layers cases by using the geological approach. In these three settings the $K_{H-average}$ and $K_{V-average}$ are the same. Scenarios with the three different CR of 10, 50 and 100. All scenarios consider buoyancy. All the parameters set for this scenario are included in Table 3.4.

Table 3.4: Hydraulic conductivities for the 1, 10 and 20 layers simulations with contrast ratios of 10, 50 and 100 under the geological approach scenarios. Layer arrangement is shown in Figure 3.3.

			High-K layers		Low-K layers	
Scenario	Layers	Contrast	K_H	K_V	K_H	K_V
C1	1	10	5	0.85	5	0.85
C2	10	10	7.81	3.91	0.78	0.39
C3	20	10	7.81	3.91	0.78	0.39
C4	1	50	5	0.2	5	0.2
C5	10	50	8.22	4.11	0.16	0.08
C6	20	50	8.22	4.11	0.16	0.08
C7	1	100	5	0.1	5	0.1
C8	10	100	8.28	4.14	0.08	0.04
C9	20	100	8.28	4.14	0.08	0.04

3.5 Impact of vertical grid resolution

The standard vertical grid cell size dz_{sr} is 1 m. We tested simulations with a higher resolution dz_{hr} of 0.5 m to make sure that the results refer to physical phenomena rather than model resolution issues. The difference between the high dz_{hr} and standard resolution dz_{hs}, dRE, is:

$$dRE = dz_{hr} - dz_{sr} \tag{18}$$

The dRE was calculated for a 10 years period, for a single-layer setting, for the 10-layer setting and for the 20-layer setting. The 10 layers case is composed of an alternation of high-K and low-K layers of 6 m and 4 m thickness, while the 20 layers case is composed of an alternation of high-K and low-K layers of 3 m and 2 m thickness. The standard deviation was calculated for each simulated setting. Results are summarized in Table 3.5 and plotted in Figure 3.4.

The single-layer setting has the smallest standard deviation and the highest difference between the aquifer thickness and the vertical grid resolution dz. Conversely, the 20-layer setting has the highest standard deviation and the smallest difference between the layer thickness and the vertical grid resolution (Table 3.5).

The standard deviations for the single-layer and the 10-layer setting are smaller than the time resolution (discrete increments of 1.10 %), but the standard deviation for the 20-layer setting is higher than the time resolution. Thus, the simulations run under the 10-layer setting are not affected by model resolution issues. The test simulations show that results are not significantly impacted by the vertical grid resolution.

Table 3.5: Comparison of RE in the $dz_{sr} = 1\ m$ and $dz_{hr} = 0.5\ m$ in a single-layer setting, 10-layer setting and 20-layer setting. Simulations were run for 10 years with a CR is 10 and a K_{H-av} of 5 m/d. RE_{sr} and RE_{hr} are the RE for the dz_{sr} and dz_{hr} simulations, respectively.

Year	**Single-layer setting**			**10-layer setting**			**20-layer setting**		
	RE_{sr}	RE_{hr}	dRE	RE_{sr}	RE_{hr}	dRE	RE_{sr}	RE_{hr}	dRE
1	61.54%	61.54%	0.00%	8.79%	8.79%	0.00%	8.79%	7.69%	-1.10%
2	64.84%	64.84%	0.00%	20.88%	21.98%	1.10%	18.68%	15.38%	-3.30%
3	65.93%	65.93%	0.00%	74.73%	74.73%	0.00%	53.85%	56.04%	2.20%
4	65.93%	65.93%	0.00%	64.84%	63.74%	-1.10%	54.95%	53.85%	-1.10%
5	65.93%	65.93%	0.00%	60.44%	60.44%	0.00%	56.04%	59.34%	3.30%
6	65.93%	65.93%	0.00%	59.34%	59.34%	0.00%	56.04%	57.14%	1.10%
7	67.03%	65.93%	-1.10%	59.34%	59.34%	0.00%	54.95%	56.04%	1.10%
8	65.93%	65.93%	0.00%	59.34%	58.24%	-1.10%	54.95%	54.95%	0.00%
9	67.03%	67.03%	0.00%	58.24%	58.24%	0.00%	54.95%	54.95%	0.00%
10	67.03%	65.93%	-1.10%	58.24%	58.24%	0.00%	54.95%	56.04%	1.10%
stdv			0.46%			0.62%			1.87%

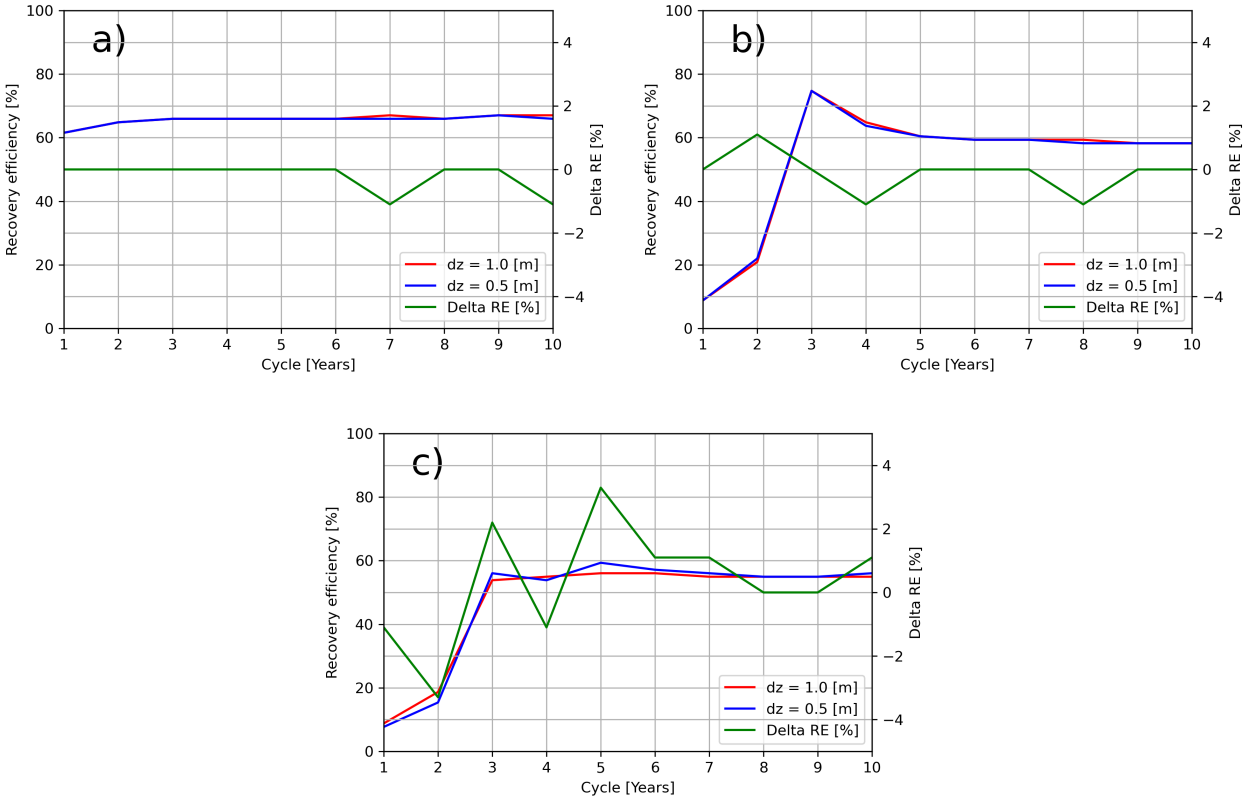

Figure 3.4: Comparison of RE in the $dz_{sr} = 1\ m$ and $dz_{hr} = 0.5\ m$: (a) single-layer setting; (b) 10-layer setting and (c) 20-layer setting.

4 Results

Results for simulations under the numerical approach and geological approach are shown in this section (Table 4.1). All simulations include buoyancy.

Table 4.1: Resultant RE over 10 cycles for the simulations listed in Table 3.3 and Table 3.4

Scenario	Year 1	Year 2	Year 3	Year 4	Year 5	Year 6	Year 7	Year 8	Year 9	Year 10
A1	8.79%	17.58%	52.75%	65.93%	58.24%	56.04%	56.04%	54.95%	54.95%	56.04%
A2	6.59%	10.99%	20.88%	19.78%	19.78%	20.88%	20.88%	20.88%	21.98%	21.98%
A3	4.40%	5.49%	5.49%	5.49%	5.49%	5.49%	5.49%	5.49%	5.49%	5.49%
A4	6.59%	14.29%	25.27%	23.08%	24.18%	24.18%	25.27%	25.27%	26.37%	26.37%
A5	1.10%	2.20%	35.16%	74.73%	59.34%	54.95%	54.95%	53.85%	53.85%	53.85%
A6	1.10%	2.20%	25.27%	23.08%	23.08%	23.08%	24.18%	24.18%	24.18%	25.27%
A7	1.10%	1.10%	19.78%	18.68%	19.78%	19.78%	20.88%	20.88%	20.88%	21.98%
A8	1.10%	1.10%	1.10%	1.10%	1.10%	1.10%	1.10%	1.10%	1.10%	1.10%
A9	59.34%	61.54%	62.64%	62.64%	62.64%	62.64%	62.64%	62.64%	63.74%	62.64%
B1	72.53%	80.22%	80.22%	81.32%	81.32%	81.32%	81.32%	81.32%	81.32%	81.32%
B2	10.99%	19.78%	27.47%	37.36%	60.44%	89.01%	91.21%	85.71%	81.32%	78.02%
B3	76.92%	89.01%	91.21%	93.41%	94.51%	94.51%	96.70%	95.60%	96.70%	96.70%
B4	54.95%	68.13%	73.63%	76.92%	78.02%	79.12%	80.22%	80.22%	80.22%	80.22%
B5	59.34%	61.54%	62.64%	62.64%	62.64%	62.64%	62.64%	62.64%	63.74%	62.64%
B6	41.76%	43.96%	45.05%	46.15%	46.15%	46.15%	47.25%	47.25%	48.35%	48.35%
B7	8.79%	17.58%	38.46%	79.12%	65.93%	60.44%	60.44%	59.34%	59.34%	58.24%
B8	28.57%	36.26%	38.46%	36.26%	34.07%	35.16%	38.46%	45.05%	52.75%	63.74%
B9	61.54%	65.93%	65.93%	67.03%	67.03%	67.03%	67.03%	67.03%	67.03%	67.03%
B10	75.82%	86.81%	90.11%	91.21%	92.31%	92.31%	93.41%	93.41%	93.41%	93.41%
B11	41.76%	43.96%	45.05%	46.15%	46.15%	46.15%	47.25%	47.25%	48.35%	48.35%
B12	73.63%	84.62%	86.81%	86.81%	87.91%	87.91%	87.91%	87.91%	87.91%	89.01%
B13	8.79%	9.89%	8.79%	10.99%	16.48%	31.87%	58.24%	80.22%	85.71%	87.91%
C1	61.54%	64.84%	65.93%	65.93%	65.93%	65.93%	67.03%	65.93%	67.03%	67.03%
C2	8.79%	20.88%	74.73%	64.84%	60.44%	59.34%	59.34%	59.34%	58.24%	58.24%
C3	8.79%	18.68%	53.85%	54.95%	56.04%	56.04%	54.95%	54.95%	54.95%	54.95%
C4	73.63%	84.62%	85.71%	86.81%	87.91%	86.81%	87.91%	87.91%	87.91%	87.91%
C5	6.59%	6.59%	9.89%	24.18%	56.04%	81.32%	89.01%	90.11%	90.11%	90.11%
C6	2.20%	4.40%	17.58%	69.23%	89.01%	91.21%	90.11%	86.81%	85.71%	84.62%
C7	75.82%	86.81%	90.11%	91.21%	91.21%	92.31%	93.41%	93.41%	93.41%	93.41%
C8	29.67%	35.16%	34.07%	36.26%	40.66%	50.55%	64.84%	76.92%	83.52%	85.71%
C9	2.20%	3.30%	9.89%	31.87%	63.74%	84.62%	91.21%	93.41%	95.60%	94.51%

4.1 Numerical approach

4.1.1 Fresh water bubble in a binary layer setting layer

The distribution of the freshwater bubble in the salt profile is described for a one-year simulation. Every phase is represented by its last day of activity, so it is possible to analyse the effects of each whole phase in the saline profile.

With buoyancy

During the injection phase, the freshwater penetrates further from the injection well in high-K layers than in low-K layers. The difference in the freshwater penetration distance between high-K and low-K layers results in 3 vertical sections: (i) the left-section, where the high-K and low-K layers are saturated in freshwater, is located closer to the injection well; (ii) the center-section, where the high-K layers are saturated in freshwater and the low-K layers are saturated in native water, is located a medium distance from the injection well; and (iii) the right-section, where the high-K and low-K layers are saturated in native water, is located further from the injection well (Figure 4.1a). The buoyancy due to density effect takes place mainly in the high-K layers, which results in interfaces with greater tilting. During the storage phase, changes in the freshwater bubble are controlled by diffusion, which results in a widening of the fresh-salt water interface and buoyancy, leading to increase tilting in the high-K layers (Figure 4.1b). During the recovery phase, the extraction of water is higher

in the high-K layers (Figure 4.1c). During the inactive phase, in the left-section, buoyancy in the low-K layers leads to an upward flow of fresh water that pushes up the brackish water at the bottom of the above high-K layers. In the center-section, buoyancy in the low-K layers does not affect the buoyancy in the above high-K layer, leading to a downward flow of saltwater in the high-K layer. The right-section is not affected by buoyancy as there is no difference in density. In the left and center-sections, the base of the low-K layers is pushed up by the underneath high-K layer freshwater.

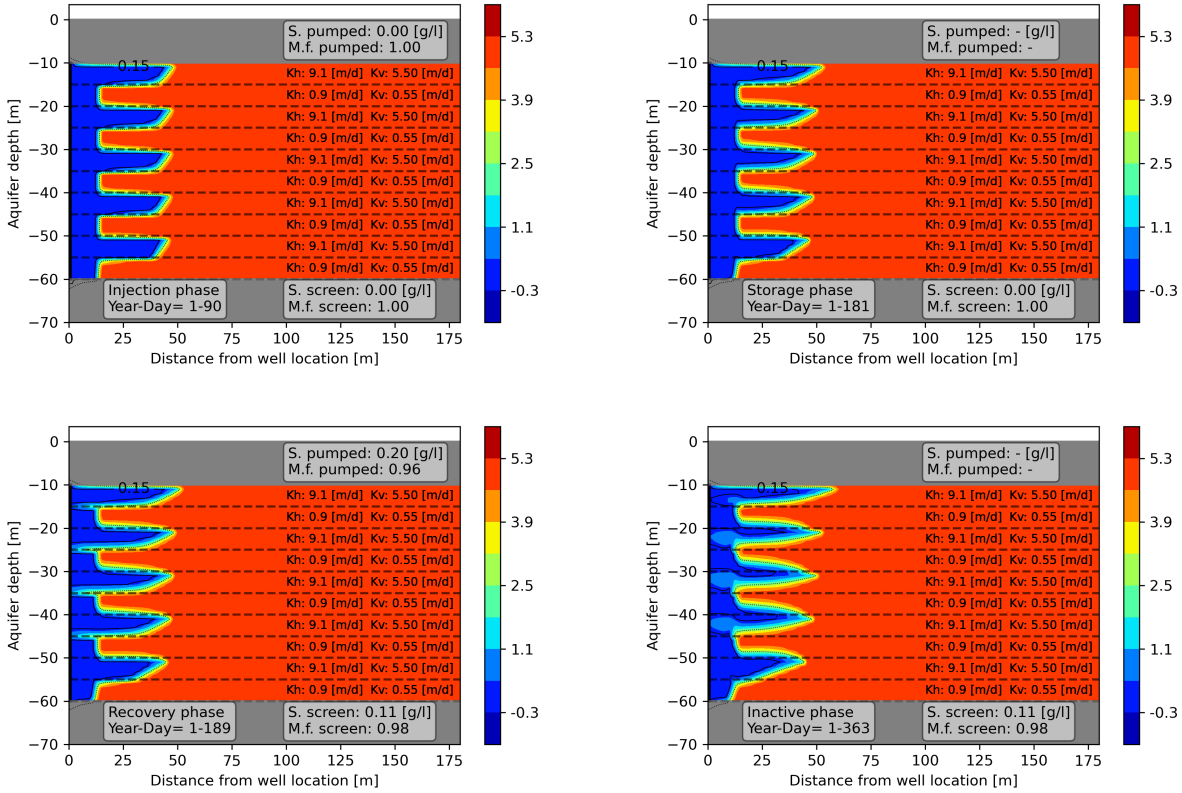

Figure 4.1: Chloride concentration profile for salinity = 5 g/l and K_{H-av} = 5 m/d scenario during the first year of simulation. (a) Last day of injection phase; (b) last day of storage phase; (c) last day of recovery phase; and (d) last day of inactive phase. Cutoff = 0.15 g/l (continuous line) and interface front = 2.5 g/l (dotted line) are shown.

Without buoyancy

For no buoyancy simulations, similarities and differences can be depicted when compared to the buoyancy simulations. On the one hand, the penetration distance of freshwater is controlled by the hydraulic conductivity of the layers. Furthermore, regarding layers of the same conductivity, the widening of the fresh-salt water interface takes place at the same ratio. Thus, there is no differentiation regarding depth and there is no tilting in the fresh-salt water interface. Nevertheless, the presence of these 3 vertical sections is irrelevant because of the absence of buoyancy (Figure 4.2).

Contact area: contrast ratios of 10 and 100

The difference in K values between layers controls the extent of the contact area between fresh and saline water as the freshwater penetration distance is controlled by the hydraulic conductivity. The higher the contrast ratio CR, the greater the contact area which means an increment in the penetration distance for high-K layers, but a decrease for low-K layers. Furthermore, the more layers are present in the profile, the bigger is the contact area and dispersion increases the mixing of fresh and saline water. Under this approach (numerical approach) this difference is bigger in the low-K layers than in the high-K layers (Figure 4.3).

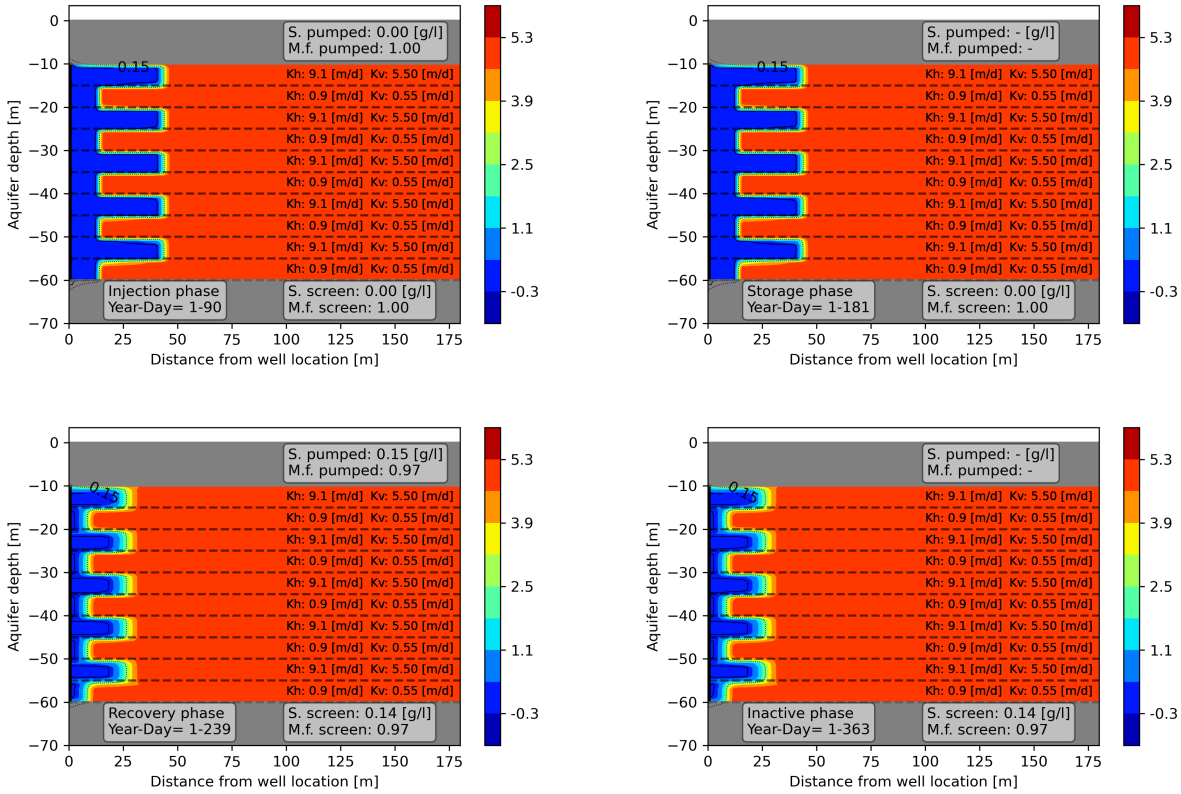

Figure 4.2: Chloride concentration profile for salinity = 5 g/l and K_{H-av} = 5 m/d scenario in a without buoyancy case during the first year of simulation. (a) Last day of injection phase; (b) last day of storage phase; (c) last day of recovery phase; and (d) last day of inactive phase. Cutoff = 0.15 g/l (continuous line) and interface front = 2.5 g/l (dotted line) are shown.

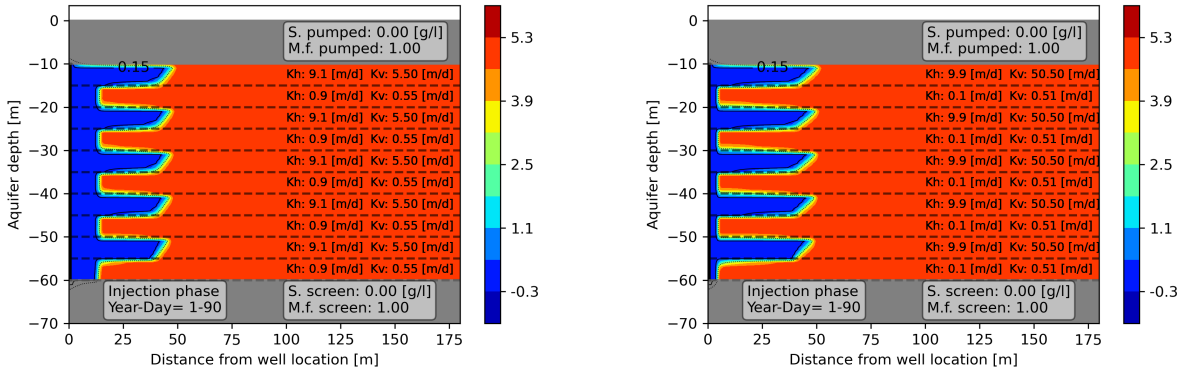

Figure 4.3: Penetration distance of injected fresh water after 1 year under hydraulic-conductivity contrast ratios of (a) 10 and (b) 100. Salinity is 5 g/l and K_{H-av} = 5 m/d.

4.1.2 Binary heterogeneous setting for 10 layers and 10 cycles

Figure 4.4a shows the RE over 10 years of simulation (RE values in Table 3.3). The simulated native water salinities C are 5 g/l and 10 g/l; the average horizontal hydraulic conductivities K_{H-av} are 5 m/d and 10 m/d and the contrast ratios CR are 10 and 100. All the simulations with a CR = 10 start with low performances (RE lower than 10%) but rapidly increase over the simulated years (Figure 4.4a). The simulations of CR = 10 have a better performance than the CR = 100 during the first 3 to 4 years, but this difference is drastically reduced for the later cycles. The best long-term performances are at the lowest salinities and hydraulic conductivities. In addition, the RE is almost null during the first 2 years for simulations of CR = 100. The RE for the same setting but without buoyancy is shown in Figure 4.4b.

Scenario C = 5 g/l and K = 5 m/d
The Figure 4.5 shows the evolution of the chloride concentration profile at the beginning of the storage phase over 10 years for the scenario of CR = 10, C = 5 g/l and K = 5 m/d. The freshwater injected in high-K layers during the first cycle flows upwards due to buoyancy through the low-K layers and appears in the above next high-K layer, where it can be easily extracted during the later extraction phases. This process results in an extra source of freshwater that improves the RE in years in years 3 and 4 (Figure 4.4a). This ascension through the low-K layers takes place in the center-section. During the first 4 years, the front of the left and center-sections are vertical. After that, the front starts to rotate and becomes diffuse. It occurs because the freshwater in the low-K layers hasn't experienced the buoyancy effect yet during the first 4 years, so the contribution of freshwater to the high-K from the low-K layers is similar in all layers. In the coming cycles, the influence of buoyancy in the low-K layers becomes more important, which results in a drop of RE. The scenario with native water salinity of 5 g/l and K = 5 m/d (blue lines in Figure 4.4a) has the highest RE.

The Figure 4.6 shows the evolution of the chloride concentration profile at the beginning of the storage phase over 10 years for the scenario of CR = 100. The difference in the penetration distance between high and low-K layers is bigger in the scenario with a CR = 100. The volume of freshwater injected in a high-K layer underneath and recovered from a high-K layer above is greater in the CR = 100 scenario This explains the greater RE at year 4 but lower RE during the first 3 years in comparison to the CR = 10 scenario. The K_v of the high-K layers is one order of magnitude greater in the CR = 10 case than in the CR = 100 case (numerical approach, Table 3.2). In the K_v of the low-K layers the values are in the same order of magnitude. This leads to an overestimation of the buoyancy in the high-K layers of the CR = 100 case. This behaviour results in a more significant increase in RE from the first year to the fourth cycle than in the CR = 10 case (Figure 4.4a).

Scenario C = 5 g/l and K = 10 m/d
The increment in hydraulic conductivity to 10 m/s results in a huge reduction in RE compared to C = 5 g/l and K = 5 m/d scenario. There is a reduction in the gap between the CR = 10 and CR = 100 scenarios but still, the RE is greater in the CR = 10 case than in the CR = 100. The peak of RE takes place at year 3 but it is about 40% lower than in the C = 5 g/l and K = 5 m/d scenario (yellow lines in Figure 4.4a).

Scenario C = 10 g/l and K = 5 m/d
The simulation of native water of 10 g/l and K_{av} = 5 m/d leads to RE about 2% lower compared to the C = 5 g/l and K = 10 m/d scenario. The peak of RE is about 20%, occurs in year 3 and later it stabilizes (green lines in Figure 4.4a).

Scenario C = 10 g/l and K = 10 m/d
The simulation with C = 10 g/l and K = 10 m/d (red lines in Figure 4.4a) has the worst performance and does not show a peak, as its RE is too low. The RE in the CR = 10 is 5%, while in the CR = 100 is only 1.1%. Notice that the minimum RE is 1.1% (not 0%) as the script is set to stop the day after overpasses the cutoff and the time resolution is 1.1%.

The comparison of RE in all scenarios shows that an increase in the average hydraulic conductivity leads to a reduction of RE. High conductivities lead to bigger effects of buoyancy, resulting in a steeper fresh-salt water interface line. The increment in the salinity of the native water means an increment of contrast with the freshwater injected which leads to a reduction of RE. The interface reaches the well sooner during the recovery phase, meaning a bigger contribution of native water to be extracted. Under the numerical approach, high contrast ratios (*i.e.* CR = 100) result in an unrealistic anisotropy factor in the heterogeneous case layers. In fact, K_V can become higher than K_H, which results unlikely under geological conditions. As a result, vertical flow is overestimated compared to real-world situations.

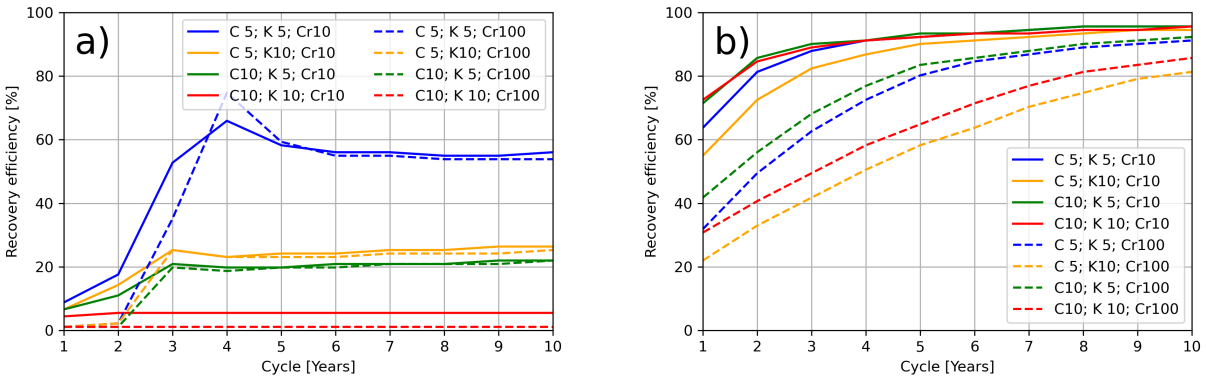

Figure 4.4: RE for variable salinities and K_{H-av} under the numerical approach over a 10 years simulation. (a) With buoyancy. (b) Without buoyancy.

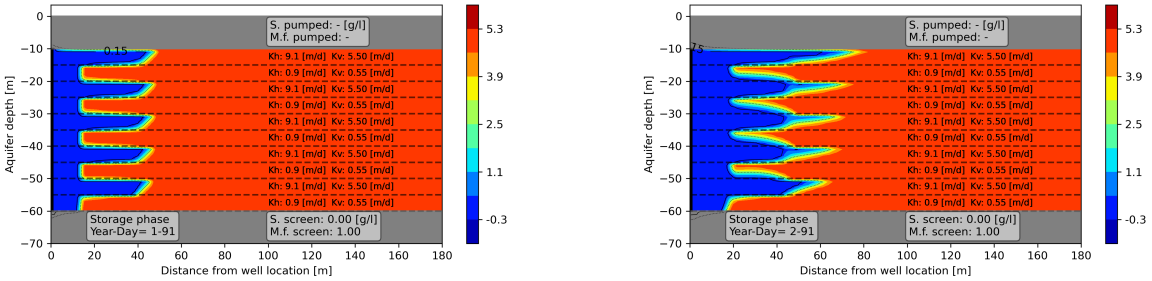

(a) Year 1

(b) Year 2

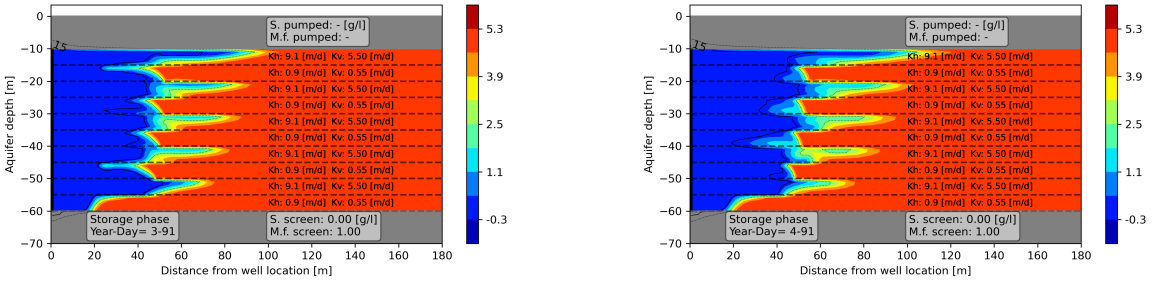

(c) Year 3

(d) Year 4

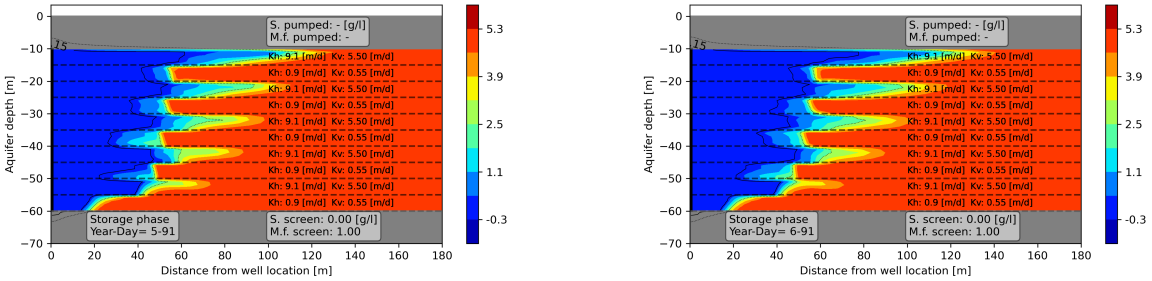

(e) Year 5

(f) Year 6

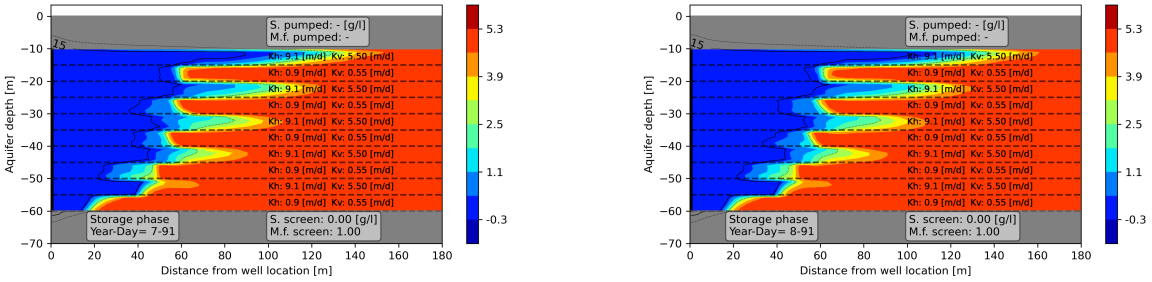

(g) Year 7

(h) Year 8

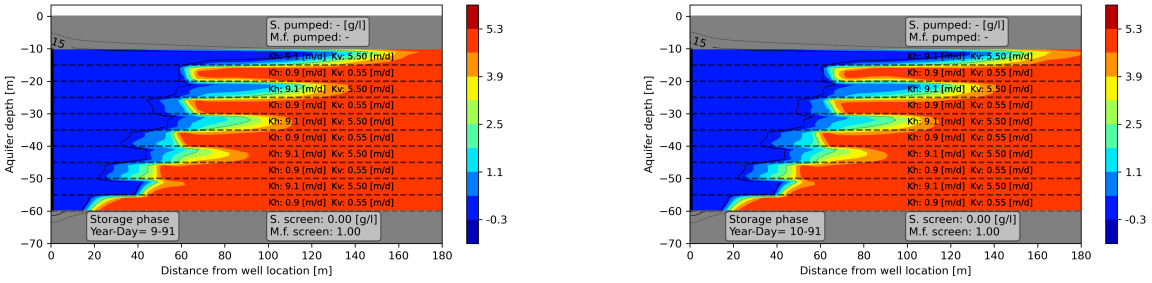

(i) Year 9

(j) Year 10

Figure 4.5: Penetration distance of injected fresh water over 10 cycles and contrast ratio 10. All profiles correspond to the 1st day of the respective storage phase. Chloride concentration profile for the native water salinity of 5 $[g/l]$, $K_{H-av} = 5$ $[m/d]$. Notice the supply of fresh water from the low-K layer into the more permeable layers in cycle 4.

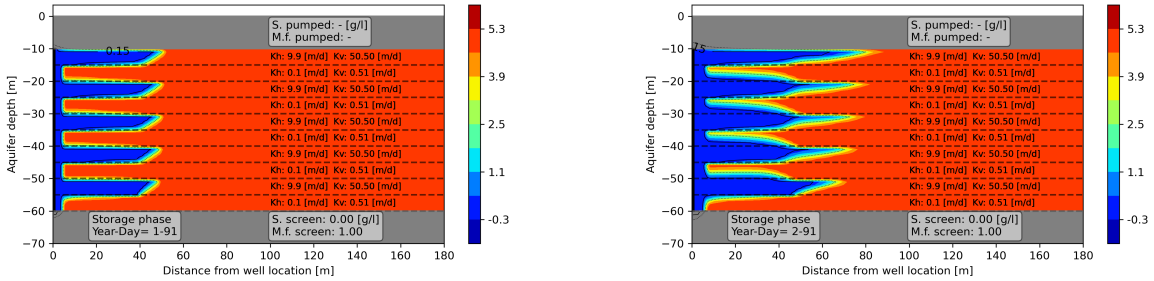

(a) Year 1

(b) Year 2

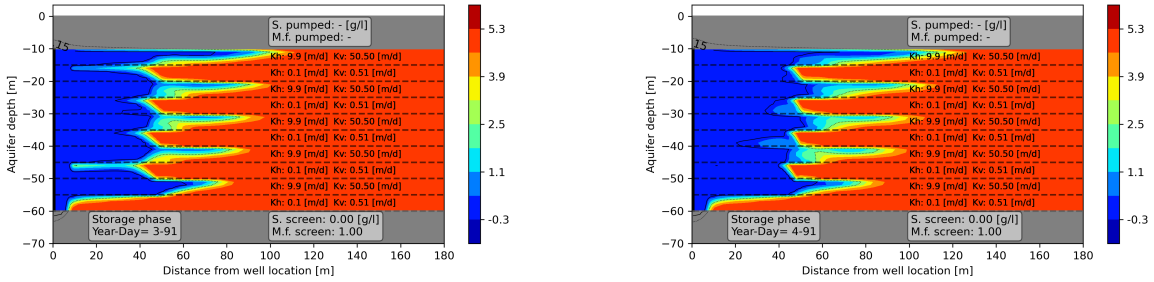

(c) Year 3

(d) Year 4

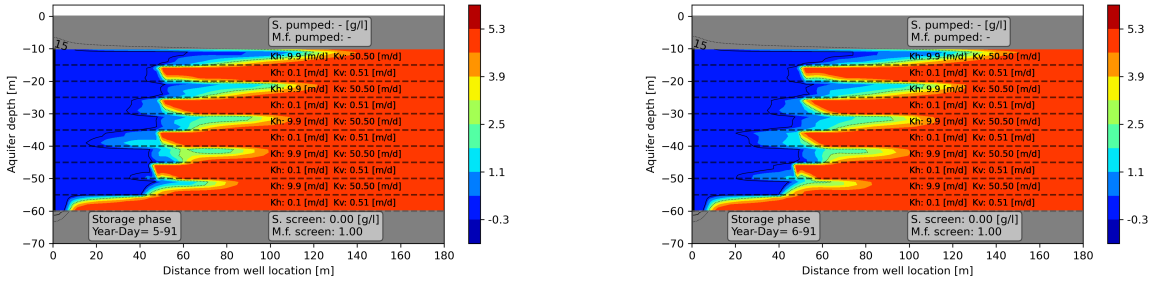

(e) Year 5

(f) Year 6

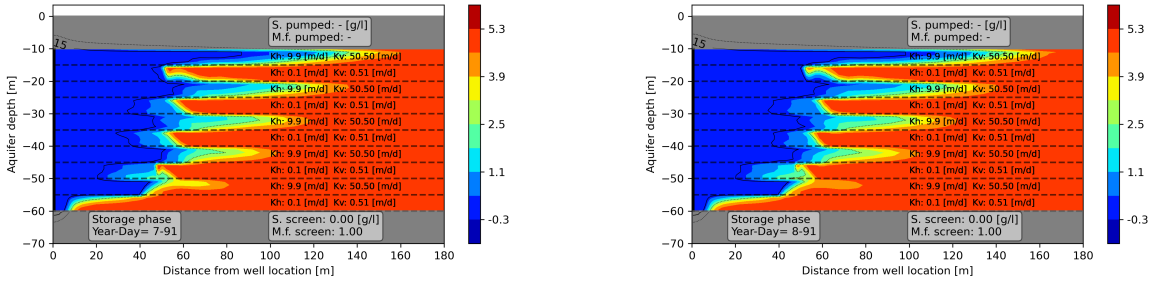

(g) Year 7

(h) Year 8

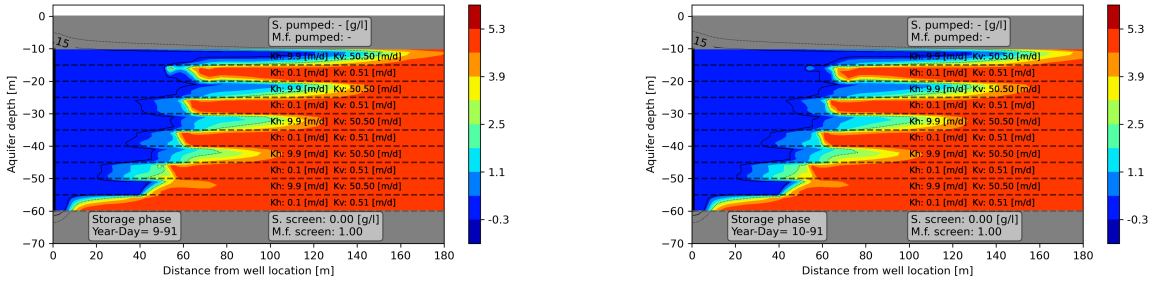

(i) Year 9

(j) Year 10

Figure 4.6: Penetration distance of injected fresh water over 10 cycles and contrast ratio 100. All profiles correspond to the 1st day of the respective storage phase. Chloride concentration profile for the native water salinity of 5 $[g/l]$ and $K_{H-av} = 5$ $[m/d]$ scenario. Notice the supply of fresh water from the low-K layer into the more permeable layers in cycle 4. CR 100 enhance the differences

4.1.3 Variable layers and variable parameters

The parameters of native water salinity, injected volume and cutoff concentrations were varied in simulations to analyze their influence on the recovery efficiency (RE). These scenarios were compared to a reference scenario with: (i) salinity 2 g/l, (ii) injected volume 50,000 m^3, and (iii) cutoff 0.15 g/l. For every scenario, one parameter is changed at a time, showing how its change affects the RE (Figure 4.7). These simulations were carried out for only 1 year because previous cases have shown that bigger differences take place after the first year of simulation.

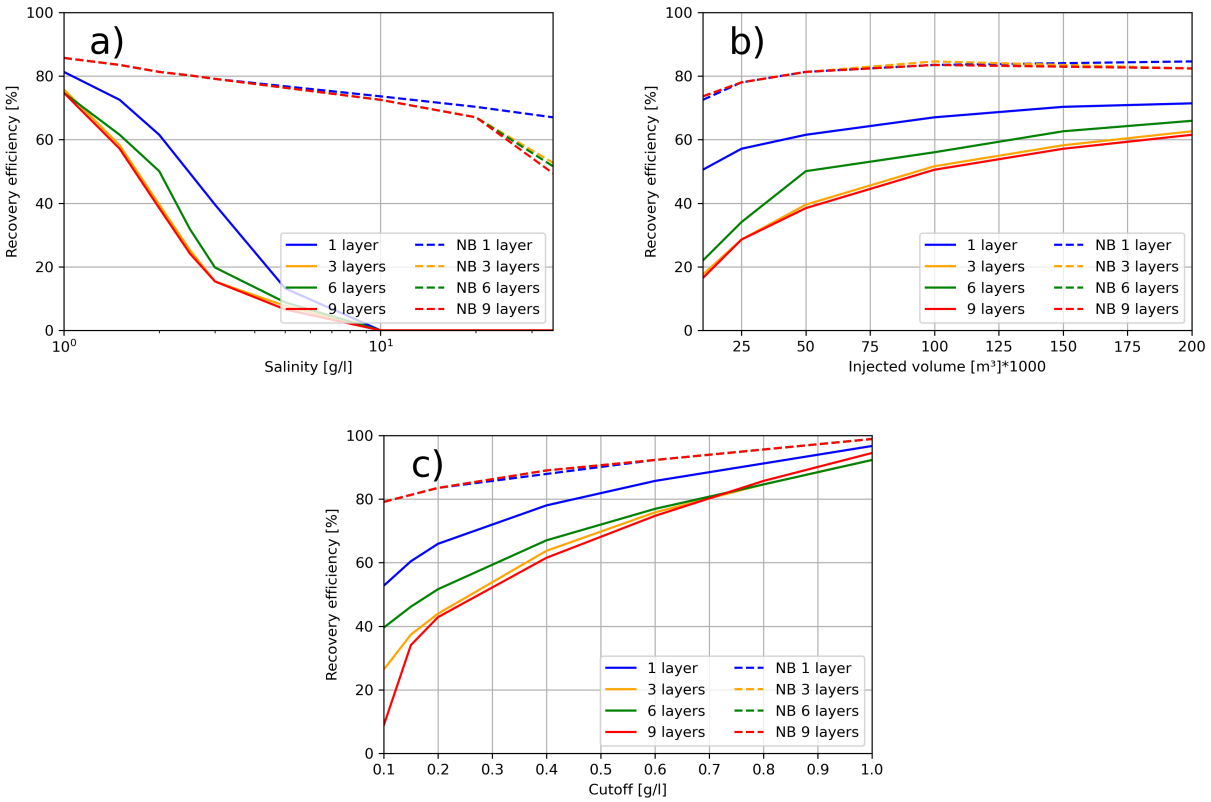

Figure 4.7: Recover efficiency for as function of (a) native water salinity; (b) injected volume and (c) cutoff concentration. Scenarios with 1, 3, 6 and 9 layers, with buoyancy (continued line) and without buoyancy (dashed lines).

Salinity
The salinity of the native water was simulated for 1, 1.5, 2.5, 3, 10 and 35 g/l (Figure 4.7a). The overall trend in RE is to decrease as the native water salinity increases. The homogeneous (1 layer) case shows a better performance than the layered (3, 6 and 9 layers) cases. The RE are noticeable for native water concentrations below 10 g/l but it is dramatically reduced to disappear at higher concentrations. Amongst the heterogeneous cases there is no big difference in RE.

Injected volume
The injected water volumes simulated are 10,000 m^3, 50,000 m^3, 100,000 m^3 and 200,000 m^3 (Figure 4.7b). There is an increase in RE as the injected volume increase. Homogeneous cases perform better than heterogeneous cases, but differences decrease when increasing injected volume. The difference between buoyancy and no buoyancy models is reduced as the amount of water injected increases.

Cutoff
The cutoff concentration simulated was: 0.1 g/l, 0.15 g/l, 0.2 g/l, 0.4 g/l, 0.6 g/l, 0.8 g/l and 1 g/l (Figure 4.7c). There is a direct relation between RE and cutoff, where the increase of the cutoff results in a better performance of the system. The homogeneous case has a better performance compared to the heterogeneous cases, while there is no big difference in the number of layers for the heterogeneous case. The difference is bigger for strict cutoffs, but it is reduced for more permissive ones.

The simulations with no buoyancy show no difference between homogeneous and heterogeneous cases. It is because of the little to no influence of dispersion-diffusion processes in the mixing of native and fresh water.

4.2 Geological approach

4.2.1 Numerical approach and geological approach

Figure 4.8 shows the RE over 10 years of simulations for the numerical and the geological approaches. The performance of the heterogeneous and its homogeneous equivalent is shown and the performance under CR of 10 and 100 is explored. The base setting is native water salinity $C = 5\ g/l$, horizontal average hydraulic conductivity $K_{H-av} = 5\ m/d$ and injected volume = 50000 m^3.

In the geological approach, the anisotropy of the heterogeneous layers is set as an independent variable in the model. This results in different values of vertical average hydraulic conductivity K_{V-av} as the parameters contrast ratio CR, horizontal average hydraulic conductivity K_{H-av}, or anisotropy factor f_{ani} change. The horizontal and vertical hydraulic conductivities of the homogeneous equivalent are identical to the horizontal and vertical average hydraulic conductivities of the heterogeneous case. So, the change in the vertical average hydraulic conductivity K_{V-av} leads to a change in the anisotropy of the homogeneous equivalent case (Table 3.2). The aim of this approach is to obtain more realistic simulations.

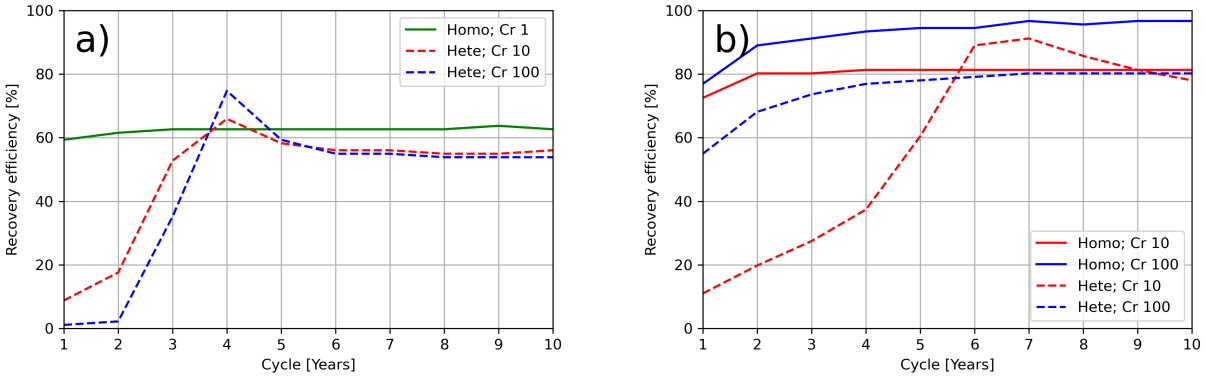

Figure 4.8: Recovery efficiency over 10 years of simulation for (a) Numerical approach. (b) Geological approach. Homogeneous equivalent (continue line) and heterogeneous (dashed line) cases are simulated for CR of 1 (green line), 10 (red line) and 100 (blue line).

Numerical approach
Under the numerical approach, the homogeneous equivalent for the CR of 10 and 100 scenarios are the same, and it is included in the Figure 4.8a. The peak of RE for the contrast ratio 10 and 100 scenarios was already explained in the previous section (Figure 4.4a).

The homogeneous equivalent starts the simulation with a high RE performance of around 60%, more than 50% higher compared to the heterogeneous cases of CR 10 and 100. The performance of the homogeneous slightly increases and stabilizes around 62% at year 3. During the first 3 years of simulation, the CR = 10 case have a better performance compared to the CR = 100 case. After year 5, the performance of the heterogeneous cases are similar and the RE of homogeneous and heterogeneous cases are relatively constant, with a better performance of the homogeneous case over the heterogeneous cases of about 8% (Table 4.1).

Geological approach
Under the geological approach, the homogeneous equivalent of the CR = 10 simulation is different to the CR = 100 simulation (Figure 4.8b and Table 3.2). The RE of the homogeneous cases is higher compared to the heterogeneous cases, both for the CR of 10 and 100 cases. The CR = 100 has a better performance than the CR = 10 simulations, conversely to the numerical approach simulations. There is a peak in RE for the CR = 10 heterogeneous case, while for the numerical approach, the RE peak is greater in the CR = 100 simulation.

This different performance regarding the numerical approach occurs due to the different values of the vertical conductivity on each case (Table 3.2). In the numerical approach, the increment in the contrast ratio results in a stronger vertical conductivity increment for the high-K layers than for the low-K layers. So, the buoyancy

under the numerical approach is controlled by the vertical conductivity of the high-K layers. This increment of vertical conductivity under the numerical approach leads to a greater effect of buoyancy in the high-K layers, which reduces the RE during the first years of simulation. On the other hand, under the geological approach, the increment of the contrast ratio CR results in a bigger reduction of the vertical conductivity in the low-K layers rather than the increase of K_V in the high-K layers. As a consequence, the amount of buoyancy in a heterogeneous profile under the geological approach is controlled by the vertical conductivity of the low-K layer, which reduces the buoyancy and improves the RE. Furthermore, the lower vertical conductivity in the low-K layers in the geological approach than in the numerical approach reduces the possibility of peaks in RE during the first years of simulations.

4.2.2 Anisotropy factor of 5 and 2 in the geological approach

The previous simulations were carried out with an anisotropy factor f_{ani} of 5, but the coming simulations use an $f_{ani} = 2$. The horizontal hydraulic conductivities in the heterogeneous layers are the same by using the f_{ani} of 2 or 5. The vertical hydraulic conductivity in the heterogeneous layers is higher when using the f_{ani} of 2 rather than the anisotropy factor of 5 (Table 3.2). The higher vertical conductivity with the anisotropy of 2 rises up the effect of buoyancy in the simulation, reducing RE (Figure 4.9). RE of the homogeneous equivalent has better performances than the heterogeneous cases, both for the anisotropy of 2 and 5.

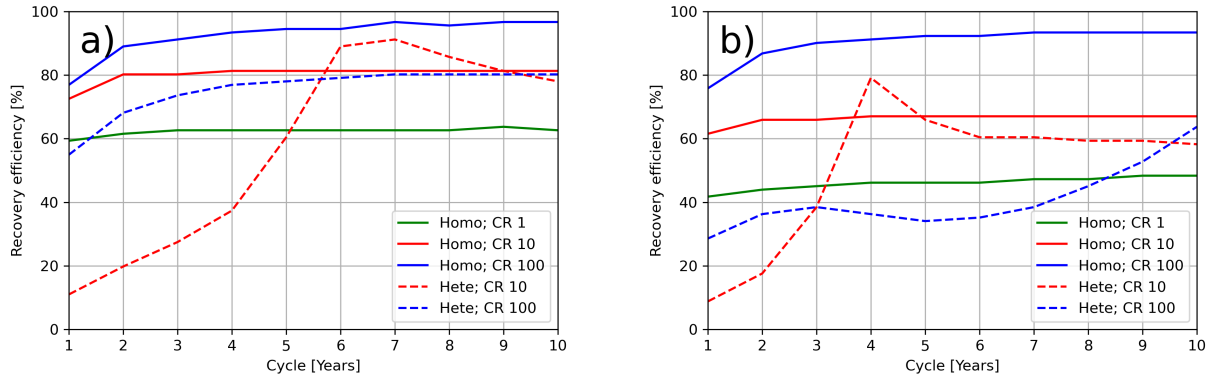

Figure 4.9: RE over 10 years of simulation using (a) Anisotropy factor of 5 and (b) Anisotropy factor of 2. It is simulated for homogeneous and heterogeneous cases under contrast ratios of 1, 10 and 100. The base scenario is native water salinity 5 g/l and K_{H-av} 5 m/d.

Anisotropy factor 5

The RE of the heterogeneous case under a CR = 10 is about 10% during the first year, rises to a peak of about 90% in the 7th year and finishes the simulation around 80%. Figure 4.10 shows the evolution of the front of the first and center-sections over time. The recovery of upward-flowing freshwater injected in the first cycle in high-K layers occurs in year 7. After that, the front of the sections starts to rotate and become diffuse. Its homogeneous equivalent start the simulation with a RE of about 75% and remains stable at around 80% after the second year of simulation. The RE of the heterogeneous case under a CR = 100 is around 55% and rises up to 80% by the end of the simulation. The RE of its homogeneous equivalent starts with a RE just below 80% and rises over 95% by the end of the simulation. The homogeneous equivalent and heterogeneous simulations under a CR = 1 are identical and have a stable RE of just over 60% during the whole simulation (Figure 4.9a).

Anisotropy factor 2

The RE of the heterogeneous case under CR = 10 is about 10%, reaches a peak of 80% in the fourth year and then decreases up to 60% until the end of the simulation. Figure 4.11 shows the evolution of the front of the left and center-sections over time. The recovery of upward-flowing freshwater injected in the first cycle in high-K layers occurs in year 4. It occurs 3 years earlier and is about 10% lower than in the $f_{ani} = 5$ case. After year 4, the front of the sections starts to rotate and become diffuse. The homogeneous equivalent of the CR = 10 case has a slight increase from around 60% to over 65% by the end of the simulation. It is about 15% lower than the $f_{ani} = 5$ case. The RE of the heterogeneous case under the CR = 100 starts around 30%, reaches a peak just below 40% in year 3, slightly decreases in year 5 and rises again after year 6, exceeding the 60% at the end of the simulation. The RE is about 20% lower and more fluctuating than the $f_{ani} = 5$ case. The homogeneous

equivalent (CR = 100) starts with a RE just below 80% and grows until 90% by the end of the simulation. Its performance is around 5% lower than the $f_{ani} = 5$ case (Figure 4.9b).

The peak in RE in the heterogeneous cases for the CR = 10 case instead of the CR 100 case, lies in the fact that CR 10 has higher vertical conductivity in the low-K layers than the CR 100 scenario (Table 3.2). The evolution of the front of the fresh-salt water in the low permeable layers can be analysed in Figure 4.10. For the homogeneous counterpart, the performance is quite similar. Thus, the CR = 1 (homogeneous case), CR = 10 and CR = 100 homogeneous equivalent start at 59.34%, 72.53% and 76.92% in the first year, and finish the simulation at 62.64%, 81.32% and 96.70%, respectively. There is a quick stabilization for all the 3 cases. Furthermore, there are no peaks in the middle of the simulation, as there are no low permeable layers that can supply delayed fresh water to the high-K layers (Figure 4.9b).

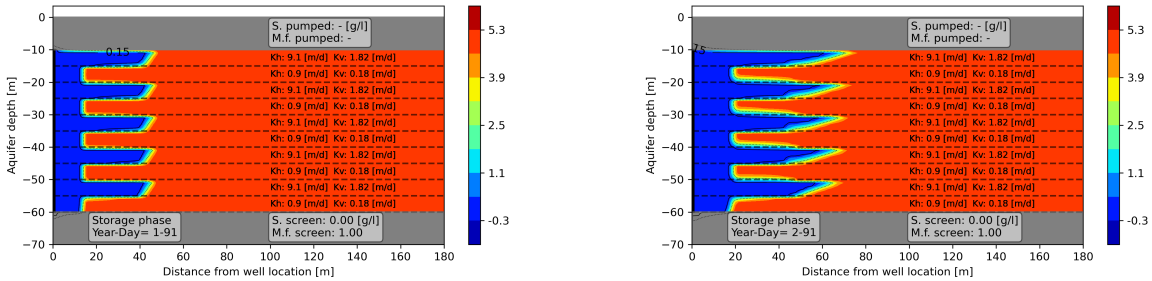

(a) Year 1

(b) Year 2

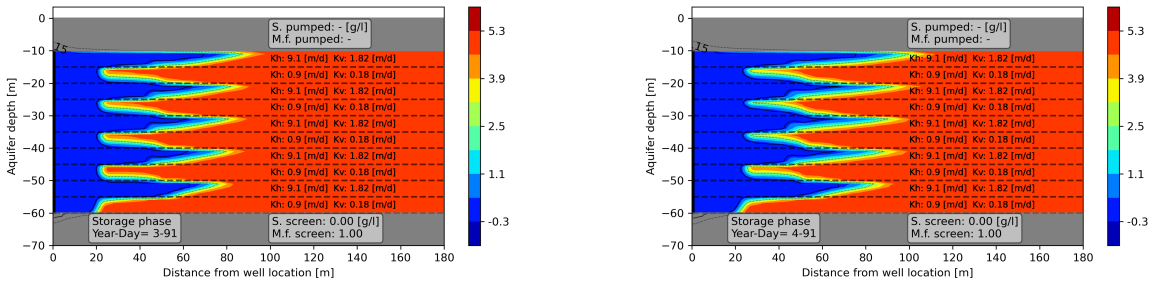

(c) Year 3

(d) Year 4

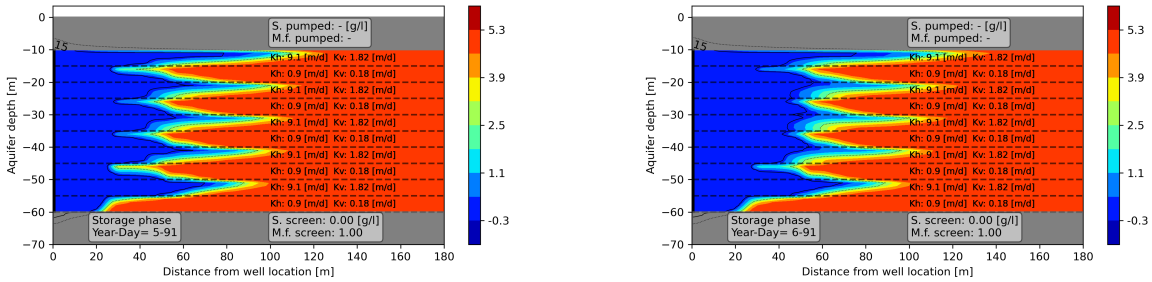

(e) Year 5

(f) Year 6

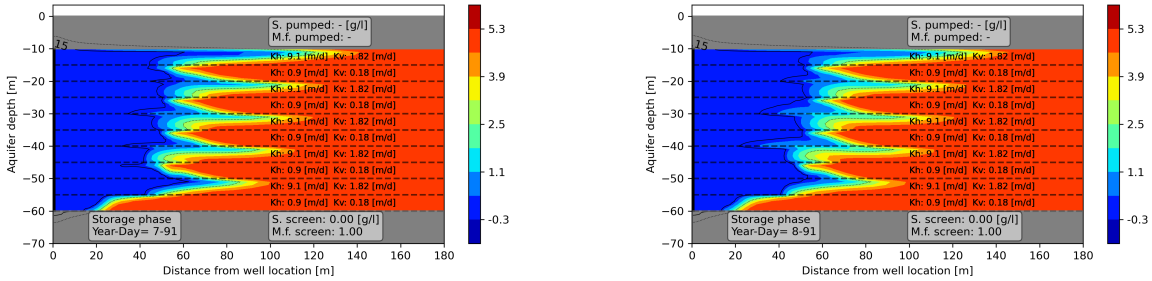

(g) Year 7

(h) Year 8

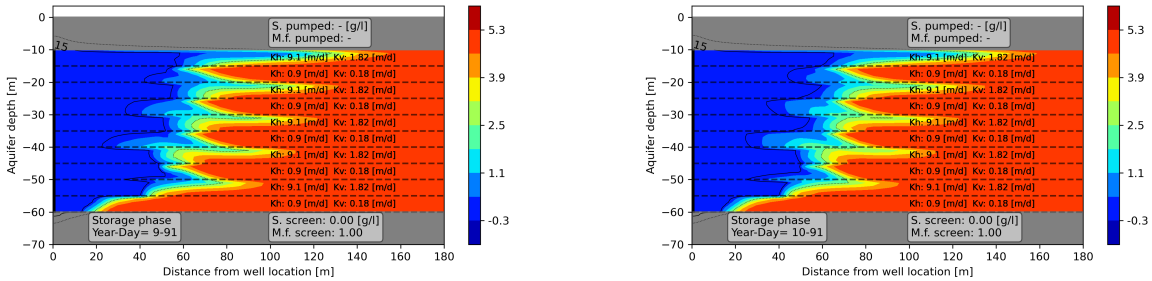

(i) Year 9

(j) Year 10

Figure 4.10: Chloride concentration profiles for the 1st day of the storage phase over 10 years. CR = 10, f_{ani} = 5, C = 5 g/l and K_{H-av} = 5 m/d.

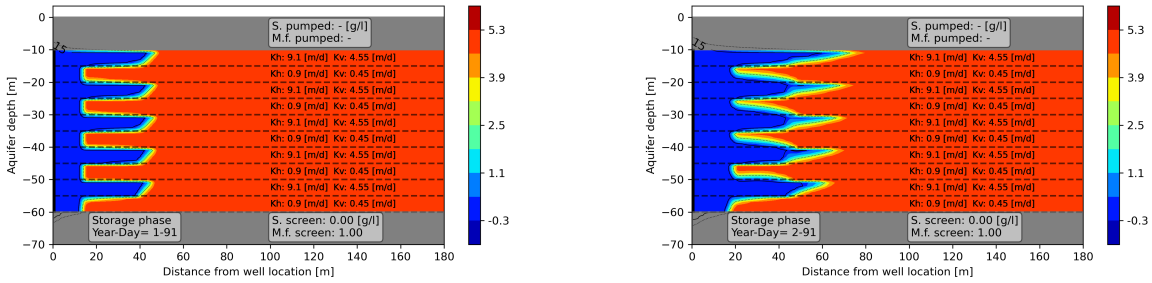

(a) Year 1

(b) Year 2

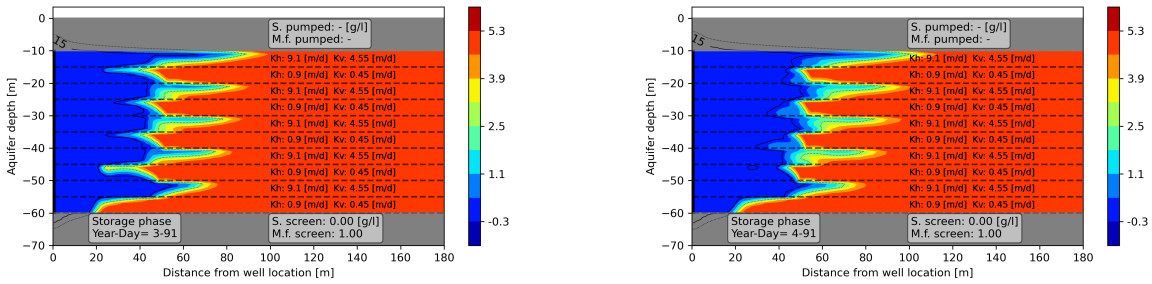

(c) Year 3

(d) Year 4

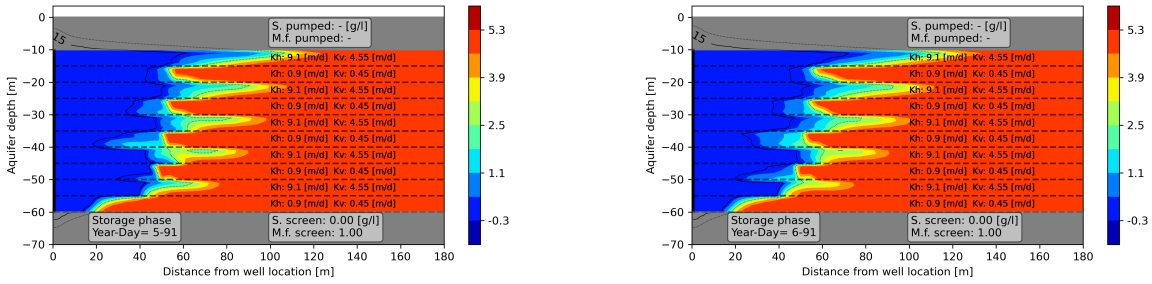

(e) Year 5

(f) Year 6

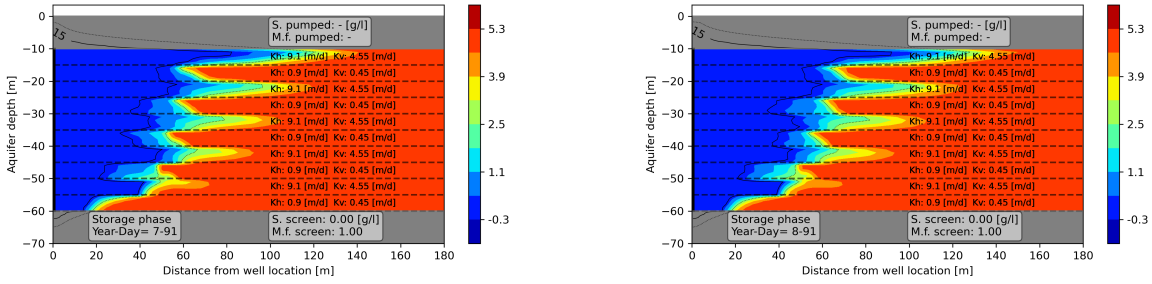

(g) Year 7

(h) Year 8

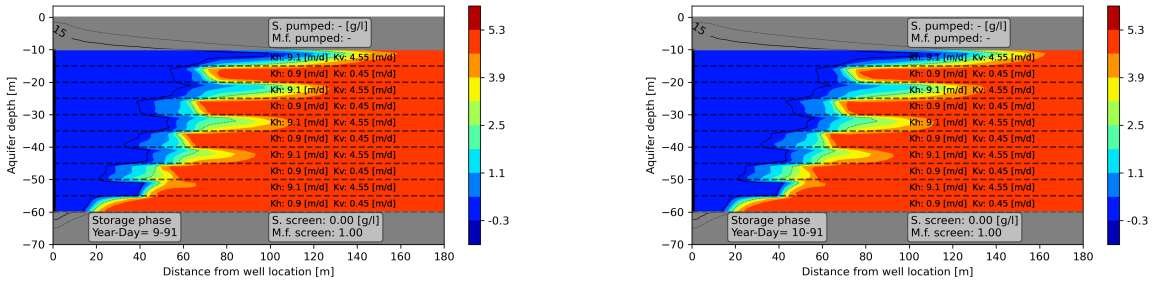

(i) Year 9

(j) Year 10

Figure 4.11: Chloride concentration profiles for the 1st day of the storage phase over 10 years. CR = 10, f_{ani} = 2, C = 5 g/l and K_{H-av} = 5 m/d.

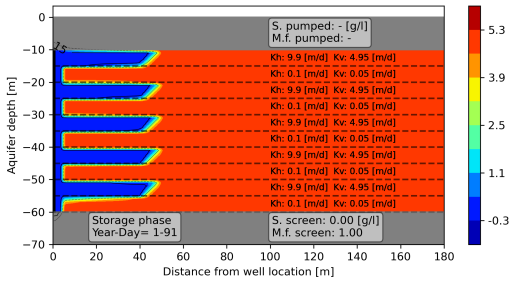

(a) Year 1

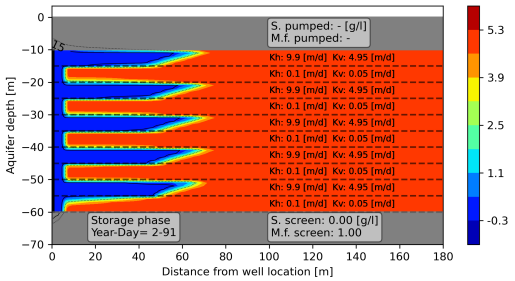

(b) Year 2

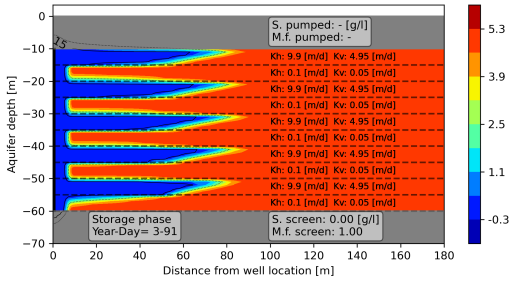

(c) Year 4

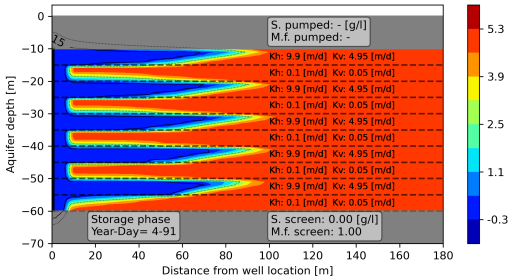

(d) Year 5

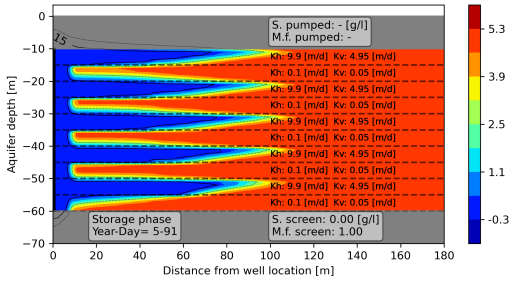

(e) Year 6

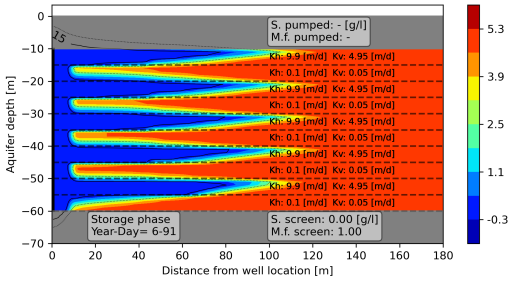

(f) Year 7

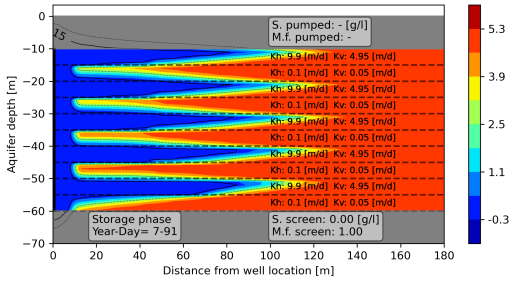

(g) Year 8

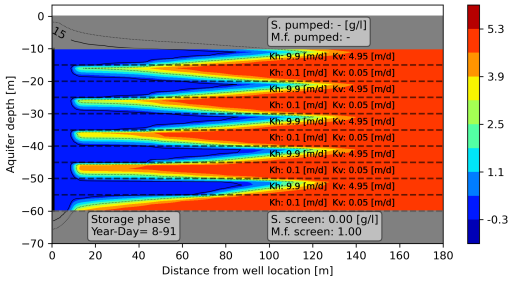

(h) Year 9

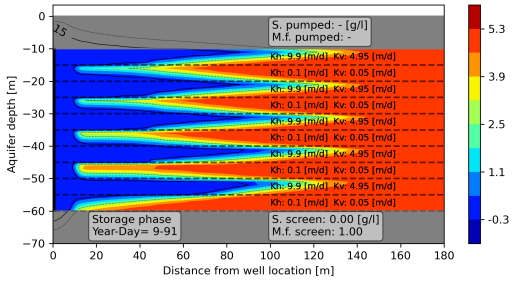

(i) Year 10

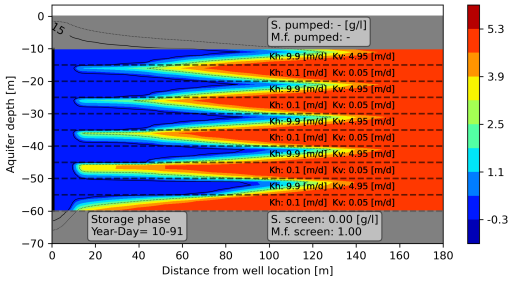

Figure 4.12: hloride concentration profiles, contrast ratio 100 and anisotropy factor 2. All profiles correspond to the 1st day of the respective storage phase. Chloride concentration profile for the Salinity 5 $[g/l]$, $K_{H-av} = 5$ $[m/d]$. Notice the "false" peak at year 3 and the later sustained increment by the end of the simulation.

4.2.3 Contact area: 10 and 20 layers

Simulations with 20 layers were carried out to explore the influence of the contact area on ASR performance. The conductivities in both cases 10 and 20 layers are the same, but the arrangement of layers is different. The thinner layers for the 20 layers arrangement mean a higher contact area than the 10 layers case, which leads to an increase in the effects of dispersion and diffusion.

In the cases of CR = 10, CR = 50 and CR = 100 the main difference in hydraulic conductivity lies on the low-K layers, where there is about 1 order of magnitude of difference between CR = 10 and CR = 100. A higher contrast ratio leads to a lower conductivity in the low-K layers, which reduces the degree of buoyancy. Conversely, the hydraulic conductivity in the high-K layers is similar have the same order of magnitude for CR = 10, CR = 50 and CR = 100 (Table 3.4).

Contrast ratio 10
In the CR = 10, the RE in the single-layer setting starts over 60% and remains stable until the end of the simulation. For the 10 layers setting, the freshwater injected in a lower high-K layer ascends through a low-K layer and shows up in the upper next high-K layer, which improves the RE in the 3rd cycle (Figure 4.13a). The latter is possible as the hydraulic conductivity in the low-K layers is the highest compared to the scenarios with higher contrast ratios (CR = 50 and CR = 100, Table 3.4). For the case of 20 layers, the RE remains relatively constant after reaching the peak in year 3. In this case, each layer is 2 times thinner than in the 10 layers case. The amount of freshwater stored in each high-K layer and the distance to overpass the low-K layers vertically during the upward flow is reduced to the half.

Contrast ratio 50 and 100
When the high contrast ratio allows the upward flow of freshwater, there is not peak developed in the middle of the simulation. It is because of the flow of freshwater in the lower high-K layer overpasses relatively fast the thin layer of low-K. As the high-K layers are thin as well, the amount of freshwater stored in them is too little, so there is not enough volume of fresh water to overpass the low-K layer. As a consequence, most of the recovered water is influenced by the surrounding native water in the high-k layers.

As the contrast ratio increases, more buoyancy occurs in the high-K layers, decreasing RE during the first years (Figures 4.13b and 4.13c) and the lowest is the low-K layer's conductivity (Table 3.4). This reduces the buoyancy for the latest stages, improving RE by the end of the simulation. Furthermore, as the conductivity in the low-K layers is the lowest, the upward flow of freshwater from one high-K layer to another is almost negligible. Thus, other processes like diffusion-dispersion become more relevant regarding mixing.

4.2.4 Salinity and hydraulic conductivity constant and different contrast ratios

Figure 4.14 shows the RE under CR of 1, 10, 50 and 100 under a base scenario of a native water salinity of 5 g/l and K_{H-av} 5 m/d. Resultant RE is shown for homogeneous equivalent and heterogeneous cases (Figure 4.14a and Figure 4.14, respectively).

1 layer
The RE under a CR = 1 scenario is high in the first year which doesn't change and stabilizes around 48%. The RE of the homogeneous equivalent for the CR of 10, 50 and 100 cases increase to around 60%, 85% and 90%, respectively (Figure 4.14a). This increment of RE as the CR increase is explained by the reduction of the vertical average hydraulic conductivity, which reduces the buoyancy and increases the RE.

10 layers
The heterogeneous cases show a fluctuating RE over time (Figure 4.14b). At a contrast ratio of 10, the RE is lower at the beginning and shows a peak in year 4. The simulation with a CR of 50 confirms this idea, as the initial RE is low due to the high buoyancy in the high-K layers. By the end of the simulation, the RE stabilizes with values as high as its homogeneous equivalent. For the CR = 100 scenario, the RE starts at higher values and has a small peak in year 3. It increases but doesn't stabilizes within the simulation time. One possible explanation is that the injected freshwater is stored at a greater distance from the well in the high-K layers. Thus, the RE is improved by the extraction of freshwater in the high-K layers, when compared to the CR of 50 and 10 cases (Figure 4.14b).

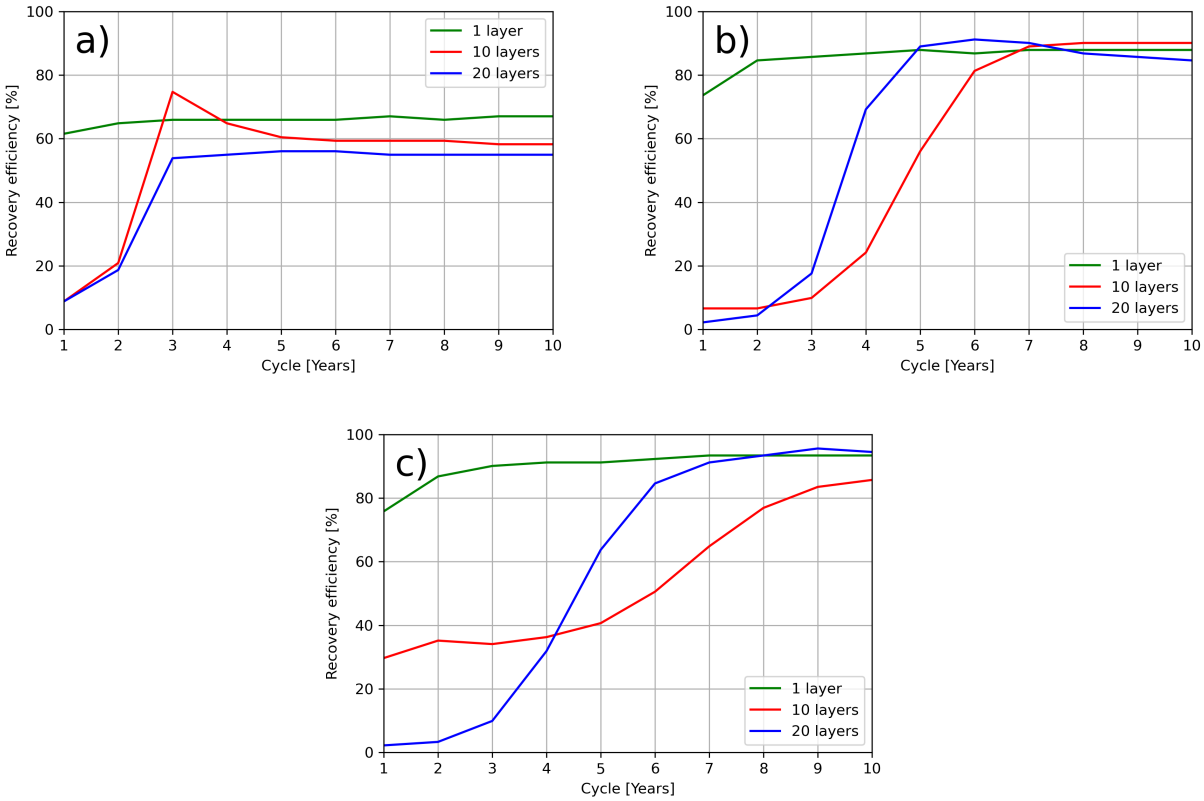

Figure 4.13: RE over 10 years for contrast ratios (a) $CR = 10$, (b) $CR = 50$ and (c) $CR = 100$. Simulations under the geological approach for 1, 10 and 20 layers using an anisotropy factor of 2.

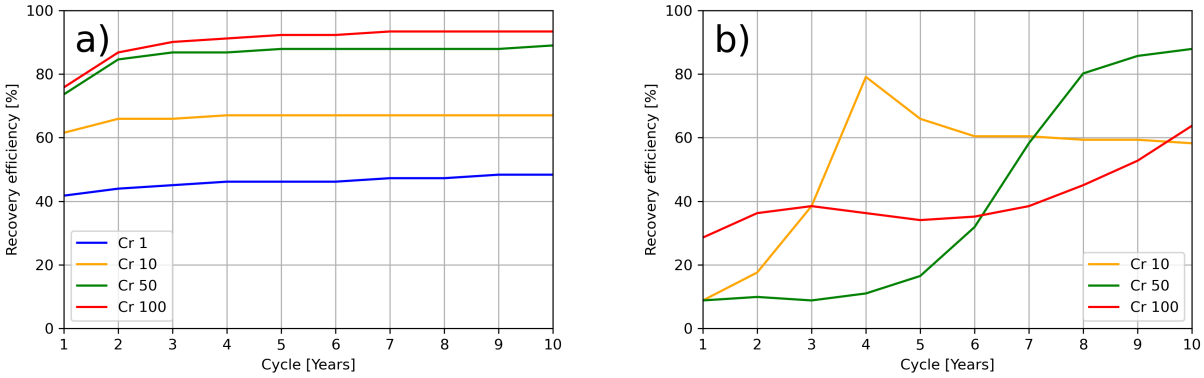

Figure 4.14: RE over 10 years for (a) Homogeneous equivalent cases and (b) heterogeneous cases. Contrast ratios of 1, 10 50 and 100 are simulated. The base case is C = 5 g/l and $K_{H-av} = 5$ m/s.

5 Discussion

Before analysing ASR systems was necessary to make homogeneous and heterogeneous settings comparable. The heterogeneity is addressed by comparing the hydraulic conductivity of the aquifer for the homogeneous and heterogeneous cases. The parameters derived from the hydraulic conductivity are the average hydraulic conductivity, anisotropy factor and the contrast ratio between the high-K and low-K layers. In this way, the defined heterogeneity ensures reproducibility by controlling the stated parameters.

The horizontal hydraulic conductivity was used to make homogeneous and heterogeneous cases comparable, where the average conductivity of the heterogeneous case is identical to the conductivity of the homogeneous equivalent case. In heterogeneous cases, the horizontal average conductivity is determined by the arithmetic mean, while the vertical average conductivity is determined by the harmonic mean. The total thickness of the aquifer is the same in both cases. For the heterogeneous cases, a binary setting of layers was defined, which means the alternation of high and low hydraulic conductivity layers (high-K and low-K layers, respectively) with a constant thickness. The total thickness of 50 m of the simulated aquifer was represented in the heterogeneous case by 5 high-K layers and 5 low-K layers, of 5 m thick each.

The horizontal average conductivity is used as an independent variable, so the values of the horizontal conductivity in each layer of the heterogeneous case became the dependent variables. The ratio between the high-K and low-K is characterized by the contrast ratio (CR) of the horizontal conductivities. Thus, two different scenarios can have the same average hydraulic conductivity but different contrast ratios. The variation in CR has a greater impact in the low-K layers than in the high-K layers, in terms of relative magnitude. The increase of one order of magnitude in the contrast ratio leads to a minimum increase in the high-K layers, but a reduction of almost one order of magnitude in the low-K layers (Figure 3.2). The use of horizontal conductivity relies on the fact that it is a measured parameter, while vertical conductivity is usually obtained from an assumed anisotropy factor, which varies according to the material and geologic aspects like granulometry and compaction. Nevertheless, vertical conductivity usually has large biases.

Two different ways to determine the vertical hydraulic conductivity are proposed: (i) the numerical approach and the (ii) the geological approach. The numerical approach uses the anisotropy of the homogeneous case as an independent variable, so the values of anisotropy in the layers that belong to the heterogeneous case become a dependent variable. Under this approach, two homogeneous cases with different contrast ratios can have the same homogeneous equivalent case, so they become numerically comparable (Figure 3.2). The increment on one-order-of-magnitude in the contrast ratio has a one-order-of-magnitude impact on the high-K layer, while in the low-K layer the increment is in a small proportion. Nevertheless, this approach lacks realism due to the overestimation of vertical conductivity in the heterogeneous layers. For instance, a CR = 100 leads to an anisotropy factor greater than 50 in the high-K layers, which means a vertical conductivity almost 5 times greater than horizontal conductivity, which is unlikely in nature. This higher anisotropy leads to an enhanced buoyancy in the high-K layers, which results in a higher contribution of brine from the high-K layers, reducing the RE.

On the other hand, the geological approach uses the anisotropy of the heterogeneous layers as an independent variable, so the average vertical conductivity (and the homogeneous equivalent vertical conductivity) is the dependent variable. This approach allows keeping the anisotropy of the layers under realistic values, as always the anisotropy is greater than 1. The increment in the contrast ratio leads to a greater impact in the low-K layers than in the high-K layers, conversely to the numerical approach. The increment of one order of magnitude in the CR leads to the reduction of one order of magnitude in the low-K layers' vertical hydraulic conductivity. In the heterogeneous case, the reduction of the vertical hydraulic conductivity of the low-K layers means a reduction in the amount of freshwater transferred from a high-K layer located below a low-K layer, to the high-K layer located above the same low-K layer. As a consequence, the system reduces its average vertical hydraulic conductivity and reduces its fluctuations in terms of RE over the simulated periods. In the homogeneous equivalent case, the increment of CR leads to a fall in the vertical hydraulic conductivity and an increase in the anisotropy. This reduction in the vertical conductivity reduces the buoyancy and the tilting of the fresh-salt water interface and improves the system's performance, compared to the numerical approach.

The difference in ASR performance between homogeneous equivalent and heterogeneous layering is clearer during the first years of simulation, where high-K and low-K layers have a greater contrast regarding the content of freshwater. At later stages, water from high-K and low-K layers in the heterogeneous cases started to mix because freshwater injected in lower layers flows up to the upper layers due to the density effect, so the overall heterogeneous performance reduces the gap regarding the homogeneous equivalent case.

When comparing homogeneous and heterogeneous cases under the geological approach, the main difference lies in the vertical hydraulic conductivity. In fact, the magnitude of the vertical conductivity can differ by 1 or even 2 orders of magnitude depending on the CR set for the heterogeneous case, while in the horizontal conductivity,

the change in the CR leads up to 1 order of magnitude of difference between heterogeneous and homogeneous equivalents. Thus, a proper selection of the anisotropy factor is key to setting realistic simulations in order to carry out realistic simulations. This selection is analyzed for every different material in the heterogeneous arrangement. Typical values of anisotropy are around 2 and 3 depending on the packing pressure and grain shape, while at an aquifer scale, it can be increased to a factor of 10 to 100 [*Beernink et al.*, 2022]. This is consistent with the simulated values, where layers with an anisotropy factor of 2 lead to an average anisotropy of 6 and 61 for the CR of 10 and 100 (Table 3.2).

In the heterogeneous cases, the transfer of fresh water from a high-K layer below a low-K layer to the high-K layer above the low-K layer is noticed (Figure 4.1d). It happens when the contrast of conductivity of layers is large enough to: (i) promote the stratification of water in the high-K layer after the recovery phase (figure 4.1c). It means the presence of freshwater in the upper section of the high-K layer while salt-water is present in the lower section of the high-K layer, and (ii) reduce the tilting in the low-K layer but allow the vertical ascent of water. In addition, the low-K should be thick enough to store fresh water to induce movement due to the density difference. The simulation shown in Figure 4.1d is set with a high-K layer on top of a low-K layer. A further simulation with a setting with the low-K on top of the high-K (the other way around) would reduce the effect of this upward flow of freshwater. Thus, we can explore whether the faster upward movement of salt water in the left-section is because of the pressure of the low-K freshwater buoyancy, or because of the inertia of the salt water movement to the left during interface tilting.

The modelling over larger periods shows a consistent increase in RE. Before starting the first cycle, the water in the ASR system is 100% of native water. Nevertheless, in later cycles, the ASR system increases the amount of freshwater not recovered during the previous cycles and reduces the proportion of native water. As the cycles are iterated, the amount of not recovered freshwater in the system increases. Thus, later cycles are analogue to one-year simulations but with a systematic increment of injected volume of water (Figure 4.7b). The increment in RE is systematic in most of the simulations. Nevertheless, some heterogeneous scenarios like A1, A5 and B7 show a peak of RE during the middle of the simulated period (Table 4.1). This peak is related to layering, where the high RE is due to the recovery of freshwater injected in previous cycles in high-K layers.

We tested the impact of various parameters on the ASR performance: salinity of the native water, the volume of injected fresh water into the system and the cutoff threshold (Figure 4.7). This analysis was carried out for a homogeneous case and the heterogeneous setting of 3, 6 and 9 layers under the numerical approach were included. There is a clear difference in performance between homogeneous and heterogeneous settings, where the homogeneous cases have a better performance than the heterogeneous cases. It is explained as the homogeneous cases under the numerical approach lead to an overestimated vertical conductivity, which results in a higher buoyancy. Further simulations under the geological approach are expected to have a better RE for the heterogeneous cases, as they mean a reduction in the vertical conductivities in the layered cases in order to keep the anisotropy constant. In the heterogeneous cases, there is not a big difference between the 3, 6 and 9 layers setting. As expected, there is a direct relationship between RE regarding injected volume and cutoff concentration, but an inverse regarding the salinity of the native water.

Simulations without buoyancy show little to no difference in the performance of a different number of layers. The almost negligible difference among different layer profiles shows that diffusion and dispersion have a very low impact. This little impact in RE is even smaller than the time resolution of 1.1% of the model.

The RE is reduced as the difference between the salinity of native water and cutoff increases, as expected. A line with the cutoff concentration is shown in the chloride concentration profiles in Figure 5.1. By the end of the recovery phase, this line is closer to the extraction well in the high-K layers of the heterogeneous cases than in the homogeneous cases. This means a higher contribution of native water to the extracted water and a reduction of RE in the heterogeneous cases. In the analyzed cases, the cutoff concentration has a value closer to the injected water than to the native water. It is, the concentration of the injected freshwater is 0 g/l, the concentration of the native water is 5 g/l and the cutoff concentration of 0.15 g/l (drinking water) results in a mixing fraction of 0.97. This mixing fraction means that only 3% of the recovered water comes from the native water and results in a better performance in the homogeneous case (RE 72.53%) than in the heterogeneous case (RE 10.99%) for the first year of simulation. A hypothetical simulation with mixing fraction of 0.5 is obtained when the cutoff concentration is equal to the middle concentration between injected and native water. It is expected that in cases where the mixing fraction is higher than 0.5, the homogeneous case will perform a better recovery efficiency than the heterogeneous case. Conversely, if the mixing fraction is lower than 0.5, the heterogeneous case will perform a better than the homogeneous case.

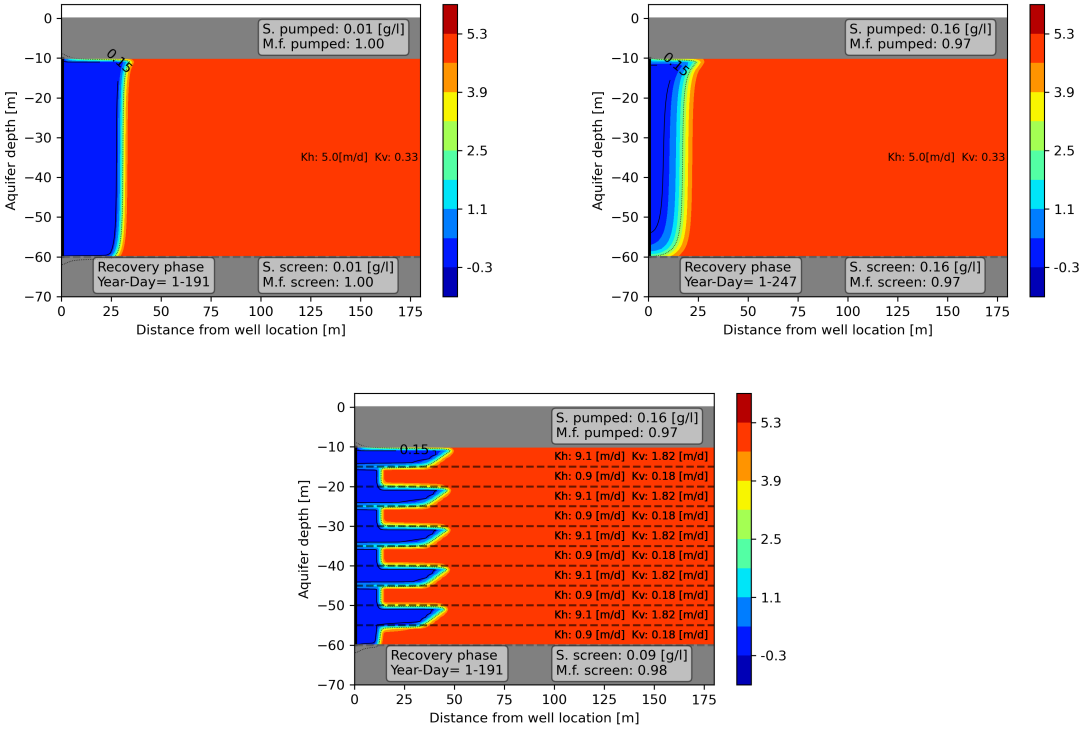

Figure 5.1: RE over 10 years for (a) Homogeneous equivalent cases at the end of the recovery phase (b) homogeneous case at the end of the recovery phase of the heterogeneous case (c) heterogeneous case at the end of the recovery phase. Geological approach, CR = 10, $f_{ani} = 5$.

6 Summary and Conclusions

The ASR system is simulated for 10 years or cycles, where every cycle consists of 4 phases: (i) injection, (ii) storage, (iii) recovery and (iv) inactive phases. The performance of the ASR systems is controlled by the recovery efficiency (RE) and it varies for homogeneous and heterogeneous cases.

Simulations were carried out by defining a homogeneous and a heterogeneous aquifer of 50 m thick where the homogeneous or heterogeneous character of the aquifer was defined in terms of the hydraulic conductivity. The heterogeneous case consisted of a binary arrangement of 10 equally thick layers where high and low hydraulic conductivity layers are alternated, high-K and low-K, respectively. The relationship of hydraulic conductivity between high and low-K was described by the contrast ratio CR. The average horizontal and vertical conductivities in the heterogeneous cases are equal to the horizontal and vertical conductivities of the homogeneous case in order to make homogeneous and heterogeneous cases comparable. The relationship between the horizontal and vertical hydraulic conductivity is described by the anisotropy factor. The anisotropy factor varies in terms of how the relationship between homogeneous and heterogeneous cases was carried out. Two different ways to define vertical hydraulic conductivity and anisotropy factor were proposed: (i) the numerical approach and (ii) the geological approach. In the numerical approach, the anisotropy factor of the homogeneous case is set as an independent parameter, while in the heterogeneous case the anisotropy of the 10 layers is set as a dependent parameter. This approach can make comparable heterogeneous with different CR, as they will have the same average hydraulic conductivity and the same homogeneous equivalent case. Nevertheless, this approach leads to unrealistic anisotropy factor when the CR is high (CR = 100). In the geological approach, the anisotropy of the heterogeneous layers is set as an independent parameter, while in the homogeneous case the anisotropy is the dependent parameter. This approach keeps realistic values for the vertical conductivity in the homogeneous equivalent and the heterogeneous case. Nevertheless, scenarios under the geological approach with different CR in the heterogeneous cases are not comparable between them, as they lead to different homogeneous equivalent cases.

Homogeneous cases have a better performance than heterogeneous cases, which is more significant during the first years of simulation. First cycles mean years 1 to 4 for the numerical approach, but up to 6 years for the geological approach, approximately. In later cycles, the gap between homogeneous and heterogeneous performances is dramatically reduced. In heterogeneous settings, the high-K layers shows higher buoyancies than the low-K layers. The penetration distance of fresh water in the high-K layers is higher in the CR = 100 case than in the CR = 10 case. The increment in native water salinity or the average hydraulic conductivity respect to the base case (native water salinity of 5 g/l, a hydraulic conductivity of 5 m/d and a contrast ratio of 10) leads to a reduction of RE. Similarly, the increment of the injected volume of freshwater and the increment of the cutoff concentration leads to an increment in the RE. Under the numerical approach, homogeneous cases have a noticeably better performance than heterogeneous cases. Heterogeneous cases with 3, 6 and 9 layers do not show a big difference in RE between them.

The geological approach shows a significant improvement in RE in comparison to the numerical approach, both for homogeneous and heterogeneous cases. In the numerical approach, the increment in CR leads to an increase of the vertical hydraulic conductivity in the high-K layers and the subsequent reduction of RE during the first cycles. In the geological approach, the increment in CR leads to a reduction of the vertical hydraulic conductivity in the low-K layers and therefore increase of RE during the first cycles. Under the geological approach, the reduction of the anisotropy factor from 5 to 2 leads to a reduction in RE due to this reduction means an increment in the vertical hydraulic conductivity.

Heterogeneous cases show fluctuations in RE over the years. Some simulations show a peak in RE around years 4 and 6. This is explained by freshwater that is injected in high-K layers during year 1 ascends through the low-K layer and later is extracted from the next high-K layer above the low-K layer. This process is more noticeable in cases where the low-K layer has a relatively high hydraulic conductivity.

Declarations

Funding: The present ASR project was kindly supported by the KWR water institute and the MSc study program supported by the *Becas Chile* program - Chilean National Agency for Research and Development ANID.

Conflicts of interests: The authors declare that the research was conducted in the absence of any commercial or financial relationships that could be construed as a potential conflict of interest.

Availability of data and code: Manuscript data and codes are included as electronic supplementary material.

References

Aldaya, M. M., A. K. Chapagain, A. Y. Hoekstra, and M. M. Mekonnen, *The Water Footprint Assessment Manual*, 0 ed., Routledge, doi:10.4324/9781849775526, 2012.

Bakker, M., V. Post, C. D. Langevin, J. D. Hughes, J. T. White, J. J. Starn, and M. N. Fienen, Scripting MODFLOW Model Development Using Python and FloPy, *Groundwater*, *54*(5), 733–739, doi:10.1111/gwat.12413, 2016.

Barker, J., Diffusion in Hydrogeology, *Diffusion Fundamentals*, *6*, 5.1 – 5.18, 2007.

Bedekar, V., E. D. Morway, C. D. Langevin, and M. Tonkin, Techniques and Methods, *Techniques and Methods*, USGS, series: Techniques and Methods, 2016.

Beernink, S., Aquifer Thermal Eneregy Storage (ATES) systems in MODFLOW/MT3D-MS/SEAWAT, Ph.D. thesis, TU Delft, 2019.

Beernink, S., A. Barnhoorn, P. J. Vardon, M. Bloemendal, and N. Hartog, Impact of vertical layering and the uncertainty and anisotropy of hydraulic conductivity on HT-ATES performance, in *European Geothermal Congress*, 2022.

Brown, C. J., J. Ward, and J. Mirecki, A Revised Brackish Water Aquifer Storage and Recovery (ASR) Site Selection Index for Water Resources Management, *Water Resources Management*, *30*(7), 2465–2481, doi:10.1007/s11269-016-1297-7, 2016.

Campisano, A., et al., Urban rainwater harvesting systems: Research, implementation and future perspectives, *Water Research*, *115*, 195–209, doi:10.1016/j.watres.2017.02.056, 2017.

Curto, D., V. Franzitta, and A. Guercio, A Review of the Water Desalination Technologies, *Applied Sciences*, *11*(2), 670, doi:10.3390/app11020670, 2021.

Elliott, J., et al., Constraints and potentials of future irrigation water availability on agricultural production under climate change, *Proceedings of the National Academy of Sciences*, *111*(9), 3239–3244, doi:10.1073/pnas.1222474110, 2014.

Essink, G., E. van Baaren, S. Galvis, K. Zuurbier, K. Raat, J. W. Kooiman, and T. Boonekamp, Potential map for large-scale implementation of subsurface water solutions: COASTAR, in *25th Salt Water Intrusion Meeting*, 2018.

Fetter, C. W., T. Boving, and D. Kreamer, *Contaminant Hydrogeology*, third edition ed., Waveland Press, 2018.

Fitts, C. R., *Groundwater Science*, Academic Press, 2002.

Guo, W., and C. D. Langevin, A Computer Program For Simulation of Three-Dimensional Variable-Density Ground-Water Flow, in *Techniques of Water-Resources Investigations 6-A7*, USGS, 2002.

Harbaugh, A. W., Techniques and Methods, *Techniques and Methods*, USGS, series: Techniques and Methods, 2005.

Kaushal, A. A., G. Krishan, and G. Pandey, Recovery Efficiency of an Aquifer Storage and Recovery (ASR) Experiment from Saline Aquifer under Controlled Conditions, *Current World Environment*, *15*(3), 441–445, doi:10.12944/CWE.15.3.07, 2020.

Kresic, N., *Hydrogeology 101: introduction to groundwater science and engineering*, Blue Ridge Press, LLC, Warrenton, 2022.

Langevin, C. D., Modeling Axisymmetric Flow and Transport, *Ground Water*, *46*(4), 579–590, doi:10.1111/j.1745-6584.2008.00445.x, 2008.

Lentz, M., Efficiently using freshwater to create a buffer zone to increase recovery efficiencies for asr systems in freshwater and brackish aquifers, *MSc internship, Utrecht University*, 2023.

Li, H., Y. Ye, and C. Lu, Aquifer Storage and Recovery in Layered Saline Aquifers: Importance of Layer-Arrangements, *Water*, *13*(18), 2595, doi:10.3390/w13182595, 2021.

Li, H., C. Lu, A. D. Werner, D. J. Irvine, and J. Luo, Impacts of Heterogeneity on Aquifer Storage and Recovery in Saline Aquifers, *Water Resources Research*, *58*(5), doi:10.1029/2021WR031306, 2022.

Lu, C., P. Du, Y. Chen, and J. Luo, Recovery efficiency of aquifer storage and recovery (ASR) with mass transfer limitation: RE OF ASR WITH MASS TRANSFER, *Water Resources Research*, *47*(8), doi:10.1029/2011WR010605, 2011.

Maliva, R. G., W. Guo, and T. M. Missimer, Hydrogeology and Aquifer Storage and Recovery System Performance, *Gulf Coast Association of Geological Societies Transactions*, *55*, 473–485, 2005.

Maliva, R. G., W. Guo, and T. M. Missimer, Aquifer Storage and Recovery: Recent Hydrogeological Advances and System Performance, *Water Environment Research*, *78*(13), 2428–2435, doi:10.2175/106143006X123102, 2006.

Molina, J. M., F. Collins, and C. M. Escobar, Fog Collection Variability in the Andean Mountain Range of Southern Colombia, *DIE ERDE*, 2008.

Page, D., L. Peeters, J. Vanderzalm, K. Barry, and D. Gonzalez, Effect of aquifer storage and recovery (ASR) on recovered stormwater quality variability, *Water Research*, *117*, 1–8, doi:10.1016/j.watres.2017.03.049, 2017.

Pandey, D. N., A. K. Gupta, and D. M. Anderson, Rainwater harvesting as an adaptation to climate change, *Current Science*, 2021.

Pavelic, P., P. J. Dillon, and C. T. Simmons, Multiscale Characterization of a Heterogeneous Aquifer Using an ASR Operation, *Ground Water*, *44*(2), 155–164, doi:10.1111/j.1745-6584.2005.00135.x, 2006.

Pyne, R. D. G., *Groundwater recharge and wells: a guide to aquifer storage recovery*, Lewis Publishers, Boca Raton, 1995.

Spang, E. S., W. R. Moomaw, K. S. Gallagher, P. H. Kirshen, and D. H. Marks, The water consumption of energy production: an international comparison, *Environmental Research Letters*, *9*(10), 105,002, doi:10.1088/1748-9326/9/10/105002, 2014.

Ward, J. D., C. T. Simmons, and P. J. Dillon, A theoretical analysis of mixed convection in aquifer storage and recovery: How important are density effects?, *Journal of Hydrology*, *343*(3-4), 169–186, doi:10.1016/j.jhydrol.2007.06.011, 2007.

Ward, J. D., C. T. Simmons, and P. J. Dillon, Variable-density modelling of multiple-cycle aquifer storage and recovery (ASR): Importance of anisotropy and layered heterogeneity in brackish aquifers, *Journal of Hydrology*, *356*(1-2), 93–105, doi:10.1016/j.jhydrol.2008.04.012, 2008.

Zuurbier, K. G., M. Bakker, W. J. Zaadnoordijk, and P. J. Stuyfzand, Identification of potential sites for aquifer storage and recovery (ASR) in coastal areas using ASR performance estimation methods, *Hydrogeology Journal*, *21*(6), 1373–1383, doi:10.1007/s10040-013-1003-2, 2013.

Zuurbier, K. G., N. Hartog, and P. J. Stuyfzand, Reactive transport impacts on recovered freshwater quality during multiple partially penetrating wells (MPPW-)ASR in a brackish heterogeneous aquifer, *Applied Geochemistry*, *71*, 35–47, doi:10.1016/j.apgeochem.2016.05.013, 2016.